



Julius-Maximilians-Universität Würzburg
Institute of Geography and Geology
Department of Remote Sensing

Master Thesis
in Applied Earth Observation and Geoanalysis

**Development of Caribbean seagrass ecosystem accounts
fusing Earth Observation with biophysical modeling of
coastal carbon**

Andrea Pilar Cárdenas Reyes

Supervisor:

Jakob Schwalb-Willmann
Universität Würzburg

Dimosthenis Traganos
Deutsches Zentrum für Luft- und Raumfahrt

Mentor:

Chengfa Benjamin Lee
Deutsches Zentrum für Luft- und Raumfahrt

Würzburg, 7th March 2024

Outline

| | |
|---|----|
| 1. Introduction | 8 |
| 2. Theory and State of the Art | 12 |
| 2.1. Background | 12 |
| 2.1.1. Carbon dynamics in seagrass ecosystems..... | 12 |
| 2.1.2. Carbon surveillance in seagrass ecosystems..... | 13 |
| 2.2. State of the Art..... | 13 |
| 2.2.1. Fundamentals of Coastal Aquatic Remote Sensing..... | 13 |
| 2.2.2. Biophysical models for carbon estimation in seagrass..... | 16 |
| 3. Study area..... | 18 |
| 4. Materials and Methods | 20 |
| 4.1. Seagrass Mapping..... | 21 |
| 4.1.1. Data sources..... | 21 |
| 4.1.2. Multi-temporal composite | 22 |
| 4.1.2.1. Mapping method of seagrass bed distribution | 26 |
| 4.1.2.2. Change detection analysis of seagrass extent | 27 |
| 4.2. Coastal blue carbon modeling (Biophysical modeling) | 27 |
| 4.2.1. Carbon estimates | 27 |
| 4.2.2. Carbon fluctuations | 30 |
| 4.2.3. Application of InVEST for Coastal Blue Carbon Biophysical Modeling.... | 30 |
| 5. Results..... | 31 |
| 5.1. Seagrass extent and change detection in the distribution of seagrass | 31 |
| 5.1.1. Classification accuracy | 35 |
| 5.1.2. Change detection in seagrass area extent | 37 |
| 5.2. Seagrass Blue Carbon Dynamics (Biophysical modeling)..... | 39 |
| 5.2.1. Estimated carbon stocks with Coastal Blue Carbon Model..... | 39 |
| 6. Discussion..... | 41 |
| 6.1. Ecosystem extension: Spatial Analysis and Temporal Dynamics of Seagrass Ecosystems | 41 |

| | |
|---|----|
| 6.2. Ecosystem condition: Health assessment of seagrass in Belize in terms of blue carbon | 43 |
| 6.3. Fusing EO with biophysical models in an EA framework..... | 45 |
| 7. Conclusion | 48 |
| 8. References..... | 49 |
| Appendix..... | 60 |

List of Figures

Figure 1. Overview of the Belize Barrier Reef Reserve System and Atolls systems. True-color Sentinel-2 imagery. Marine protected areas (MPAs) are displayed in orange, and UNESCO (2023) World Heritage Sites are in green. Three atolls (Turneffe, Lighthouse, and Glover’s Reefs) are outside the BBRRS (Gibson et al., 2004). 18

Figure 2. Process of generating a classification of benthic habitat maps from a single image composite for each period. 20

Figure 3. Training TD data distribution throughout the AOI..... 22

Figure 4. Classification results of all classes in the Belizean Marine environment using the random forest algorithm on the PlanetScope composites 32

Figure 5. Classification results of all classes in the Belizean Marine environment using the random forest algorithm on the Sentinel-2 composites 32

Figure 6. Seagrass extension in the Belizean Marine environment using the random forest algorithm on the Sentinel-2 composites..... 33

Figure 7. Seagrass extension in the Belizean Marine environment using the random forest algorithm on the PlanetScope composites..... 34

Figure 8. Changes in substrate cover from 2016 – 2022 for seagrass and coral. (=loss, = gain and = no change). Done with PS(a) and S2 (b) maps..... 38

List of Tables

| | |
|---|----|
| Table 1. Source of training points | 22 |
| Table 2. Composite details. Number of single scenes for S2-L1C and quads for NICFI Basemaps utilized for constructing the composite image. | 23 |
| Table 3. Rrs Sentinel-2 L1C and NICFI composites characteristics..... | 26 |
| Table 4. Data Sources for Estimating Metrics in the InVEST Blue Carbon Biophysical Model | 29 |
| Table 5. Data Sources for Carbon Pools for Estimating Metrics in the InVEST Carbon Storage and Sequestration Model | 29 |
| Table 6. Seagrass Coverage Area in Square Kilometers Determined for Each Image Composite..... | 33 |
| Table 7. Classification results of all classes in the Belizean Marine environment using the random forest algorithm | 34 |
| Table 8. Accuracy of RF model for seagrass maps | 36 |
| Table 9. Gains and losses for each classification map | 37 |

Abbreviation

| | |
|----------------|--|
| ACA | Allan Coral Atlas |
| BBRRS | Belize Barrier Reef Reserve System |
| CBC | Coastal Blue Carbon |
| C | Carbon |
| EEZ | Economic Exclusive Zone |
| EO | Earth Observation |
| GEE | Google Earth Engine |
| GHG | Greenhouse Gas |
| MPA | Marine Protected Area |
| NICFI | Norway's International Climate and Forests Initiative Satellite Data Program |
| OC | Organic Carbon |
| PS | PlanetScope |
| Rrs | Below-surface remote sensing reflectance |
| SEEA-EA | System of Environmental Ecosystem Accounting |
| S2 | Sentinel-2 |

Abstract

Understanding the distribution and changes in seagrass is a prerequisite for determining its carbon content and implementing conservation projects. In this study, using remote sensing techniques, the distribution and abundance of blue carbon in the seagrass meadows of the Economic Exclusive Zone (EEZ) of Belize was mapped between the years of 2016 - 2019 and 2020 - 2022 . This was done using multitemporal composite images from the Sentinel-2 Level-2C Surface Reflectance Archive and basemaps from the PlanetScope images processed through the Google Earth Engine (GEE) cloud computing platform. The mapping efforts discovered a loss in seagrass extension all over the study area. This pattern of loss was identified in both classification maps. The biophysical modeling results are based on the Coastal Blue Carbon model by InVEST. We incorporate the results from the first step into this model, using literature review data on biomass, soil carbon, accumulation rates, and net sequestration as reference carbon data. This analysis gave us a first estimate of the carbon content in terms of carbon stocks and total net carbon sequestration in Belize. Finally, we discuss the implications of fusing satellite imagery with models by comparing the efficacy of two remote sensing satellites with different spatial resolution in assessing carbon stocks within seagrass ecosystems. The results show a significant increase in carbon stock from 53.91 Mt CO₂e/ha in 2016 to 2019, to 128.52 Mt CO₂e/ha in the years of 2020 to 2022.

1. Introduction

Seagrass meadows are among the so-called blue carbon ecosystems that have the potential to store large amounts of organic carbon in their soils for long periods (Atwood et al., 2020). Seagrasses are angiosperm marine plants found in temperate, subtropical and tropical regions (Duarte, 2002). They are globally distributed in 191 countries across tropical and temperate seas (F. Short et al., 2007).

Seagrass habitats play an important role in shallow coastal areas by providing essential ecosystem services (do Amaral Camara Lima et al., 2023) (Veettil et al., 2020). Among the benefits provided by these ecosystems are: providing breeding and nutritional sites for aquatic life, preventing erosion, promoting sediment deposition, contributing to food webs, and reinforcing shoreline stability (Pham et al., 2019) (Kennedy et al., 2010) (Hemminga & Duarte, 2000) (Hendriks et al., 2008).

Seagrasses have been recognized for their significant long-term carbon storage and sequestration capacity (Laffoley & Grimsditch, 2009) (Mcleod et al., 2011) (do Amaral Camara Lima et al., 2023). They accumulate carbon through excess photosynthetic carbon fixation, stored directly in sediments in their roots and rhizomes (Duarte & Cebrián, 1996). The ability of seagrass meadows to receive carbon from other sources outside their boundaries significantly increases their carbon sequestration. Hence, these marine-coastal environments store more carbon than terrestrial environments (Simpson et al., 2022) (Fourqurean et al., 2012).

Recent research has identified a global decline in seagrass habitats, threatening the wide range of benefits they provide (Veettil et al., 2020). Anthropogenic activities, including water pollution and harmful fishing methods, have precipitated a marked reduction in their geographic distribution (Duarte, 2002) (Hemminga and Duarte, 2000). In addition, factors related to climate change, such as ocean warming and sea level rise, have harmed these ecosystems (Grech et al., 2012). Findings from Waycott et al. indicate that, since 1980, the rate of decline for seagrass has been 110 km² yr⁻¹, with 29% of the world's seagrasses being destroyed.

The loss of seagrass represents a significant decline in the ecological and economic value of coastal ecosystems (C. M. Duarte, 2002). The decline or potential disappearance of seagrass ecosystems can lead to significant damage and complexities, especially considering the multitude of services they provide to coastal communities and ecosystems

worldwide (Veettil et al., 2020). Therefore, establishing seagrass distribution and abundance for climate change mitigation and coastal zone management is important.

Satellite images have proven to be a valuable tool for studying coastal and marine ecosystems. Through remote sensing, it is possible to establish the distribution and spatial extent of seagrass meadows, the percentage of geographic coverage and species composition (Stankovic et al., 2021) (Traganos & Reinartz, 2018a) (Simpson et al., 2022) (Lee et al., 2023). In addition, it makes it possible to study remote coastal and marine habitats across expansive scales (Pham et al., 2019) (Bai et al., 2023).

To assess the condition of aquatic environments, additional inputs are necessary to evaluate key elements (Simpson et al., 2022). Satellite imagery technology cannot directly measure these biophysical characteristics, necessitating alternative measurement techniques (Ibid). Integrating satellite imagery with biophysical models significantly aids in the estimation of seagrass carbon mapping, providing a pathway to estimate carbon dynamics within these species

Biophysical modeling in an ecosystem accounting framework provides spatially explicit information on carbon stocks that complements the data available and takes into account spatiotemporal heterogeneity and unpredictability of the seabed (United Nations, 2022). Therefore, biophysical models refine seagrass estimates by analyzing seagrass health, coverage and environmental factors to assess carbon content indirectly.

One of the main challenges in modeling seagrass carbon is the variation in biomass and growth rates among species (Hemminga and Duarte, 2000). This variability poses a challenge in generating accurate global estimates that can be applied to local dynamics (Serrano et al., 2021). It also impedes the optimal use of seagrass ecosystems to support nature-based solutions initiatives (do Amaral Camara Lima et al., 2023) and their incorporation into Nationally Determined Contributions (NDCs) (Arkema et al., 2023). Therefore, it is necessary to establish methodologies that can translate measurable characteristics into biophysical proxies capable of capturing the heterogeneity of seagrass ecosystems (Serrano et al., 2021).

Three major gaps remain in the effort to estimate ecosystem carbon sequestration service. First, existing methods for estimating the extent of seafloor habitats are limited to analyzing single satellite imagery and thus need more computational capacity to compare their performance. Second, a more comprehensive mapping of ecosystem changes, including understanding their temporal dynamics, is needed. Finally, a better understanding of how

carbon is stored and varies over time is needed to improve the valuation process, considering the stability of carbon storage and release mechanisms in these ecosystems.

This study aims to establish a foundational framework for incorporating blue carbon into country-specific seagrass carbon stocks and sequestration estimates at the local scale. To this end, three main objectives are proposed.

1. Investigate the spatial distribution dynamics of seagrasses within Belizean marine environments, analyzing changes across two distinct time frames: 2016-2019 and 2020-2022.
2. Employ the InVEST Coastal Blue Carbon (CBC) model to quantify the carbon content of Belizean seagrass beds.
3. Compare the efficacy of two remote sensing satellites PlanetScope and Sentinel-2, in assessing carbon stocks within seagrass ecosystems.

In doing so, we seek to raise awareness of the benefits of including seagrasses in the Nationally Determined Contributions of countries by improving existing large-scale datasets, generating national-scale data, and improving the quantification of biophysical parameters of seagrasses in the Belize BBRRS.

The Economic Exclusive Zone (EEZ) of Belize was chosen as a research area due to its significant progress in including seagrasses within its NDCs and developing a National Seagrass Management Policy. These include updating seagrass maps and identifying key areas to strengthen protection to advance sustainability initiatives.

This study uses remote sensing methodologies to accurately map the distribution and abundance of blue carbon in the seagrass meadows of the BBRRS of Belize at two epochs. Images from the Sentinel-2 Level-2C Surface Reflectance Archive and basemaps from the Norwegian International Climate and Forest Initiative (NICFI) were processed through the Google Earth Engine (GEE) cloud computing platform. Moreover, a scientific literature review collected data on the biophysical values of Belize's BBRRS seagrass carbon stocks.

Our study is composed of four main sections. The first part outlines the theoretical framework of remote sensing in coastal aquatic ecosystems and biophysical carbon models. The methodology is then divided into two key steps. The first step involves mapping seagrass meadows in Belize using two types of composites created with NICIF and Sentinel 2 imagery. This phase results in four maps, two for each type of satellite, in two-time frames: epoch 1: 2016-2019 and epoch 2: 2020-2022. The second stage involves

using these inputs within the biophysical blue carbon model and literature data to estimate the amount of carbon stored during this time period. The results of our study are then presented and analyzed in relation to the two elements of the SEEA-EA framework, ecosystem extension and condition, the optimal parameterization of the model used, and its limitations.

2. Theory and State of the Art

This chapter explores seagrass carbon research and remote sensing systems within coastal aquatic ecosystems. The first section focuses on the carbon dynamics within seagrasses and the crucial data on seagrass carbon content for understanding their role in the carbon cycle. The second section delves into the theory that will be applied in this research, highlighting the significance of satellite imagery as a proxy for carbon identification, the fundamentals of remote sensing in aquatic ecosystems, and the impact of the water column on the satellite return signal. Finally, we conclude by discussing how biophysical models contribute to a more thorough understanding of the natural processes within this aquatic ecosystem.

2.1. Background

2.1.1. *Carbon dynamics in seagrass ecosystems*

Coastal habitats accumulate organic carbon OC mainly in their sediments (Duarte et al., 2005). In particular, seagrass transforms carbon dioxide into organic carbon by filtering particulate particles from the water column (Garrard & Beaumont, 2014) and then burying OC in the sediment around their meadows by their roots and rhizomes (Johannessen, 2023) (Duarte & Chiscano, 1999). The soil presents up to 98% of the total carbon stock of seagrass ecosystems (Serrano et al., 2019). This OC stored within its sediments can remain for extended periods of time if undisturbed (Mcleod et al., 2011).

Seagrass mainly stores carbon by the allochthonous sediment trapped in its meadow., which refers to the carbon originating from outside the meadow (Johannessen, 2023). The amount of organic matter buried in seagrass sediments depends on several environmental factors, including geographic location, depth, turbidity, sediment type, sediment accumulation rate, and oxygen availability (Mazarrasa et al., 2021) (Hemminga & Duarte, 2000) (Lavery et al., 2013). Additionally, seagrass morphology and patch density can enhance carbon intake due to low decomposition rates in anaerobic seagrass sediments (Qiu et al., 2014). The lignin content on seagrass rhizomes also slows down microbial degradation, facilitating long-term carbon accumulation (Hemminga & Duarte, 2000).

It is reported that the percentage of deposited carbon buried in coastal sediments is more than 50% (Hemminga & Duarte, 2000). Seagrass contributes to 27 to 44 Tg C yr⁻¹ carbon burial rates, which account for 10 to 18% of oceanic carbon burial (Kennedy et al., 2010). Moreover, net production (NEP) refers to the amount of C that has been gained or lost within a year. This is determined by whether C is accumulating, resulting in positive net

2. Theory and State of the Art

sequestration, or being emitted, resulting in negative net sequestration (Natural Capital Project, 2024). On average, seagrasses transfer 24.3% of their NEP to neighboring ecosystems (Duarte & Cebrián, 1996), and their annual net production is 0.6×10^{15} gC per year (Duarte & Chiscano, 1999).

In recent years due to the degradation of this ecosystem, the C stocks stored by them are vulnerable to being released back into the atmosphere in the form of CO₂, thus becoming a carbon source and contributing to global warming (Mcleod et al., 2011) (Atwood et al., 2020). The amount of aboveground biomass lost, and the degree of soil modification depends on the magnitude of the disruption. As the degree of disturbance increases, more soil carbon is exposed to oxygen, leading to oxidation and subsequent CO₂ emissions (Natural Capital Project, 2024).

2.1.2. *Carbon surveillance in seagrass ecosystems*

The primary means of monitoring carbon stored in seagrasses involves in-situ observations. Typically, carbon stocks in a meadow are assessed by taking cores that capture each component, such as above-ground biomass (AGB), below-ground biomass (BGB), and soil carbon (Macreadie et al., 2014). Among the various biophysical parameters, the carbon burial flux is the most significant factor for additional carbon storage potential, while the carbon stock parameter is used for quantifying and mapping carbon that may be at risk of future release due to physical disturbances or climate change (Johannessen, 2023).

2.2. State of the Art

2.2.1. *Fundamentals of Coastal Aquatic Remote Sensing*

In recent years, spaceborne remote sensing has become extensively utilized for global surveillance of blue carbon ecosystems (Serrano et al., 2021) (Roelfsema et al., 2013). The remote sensing of seagrass includes passive and active remote sensing and LiDAR (Veettil et al., 2020) (Bai et al., 2023). In particular, multispectral and hyperspectral optical imagery have been extensively used to map this blue carbon ecosystem (Lee et al., 2023), observe long-term changes on a larger scale (Pham et al., 2019), differentiate vegetative it from other habitats (Schill et al., 2021), and monitor seagrass coverage (Blume et al., 2023), having outstanding outcomes.

Seagrasses are typically found in coastal areas in intertidal or subtidal zones, where tidal waters frequently submerge them (Bai et al., 2023). The presence of water as an additional medium affects the path of light in distinct ways, differing from its behavior in the

2. Theory and State of the Art

atmosphere (Roelfsema et al., 2009). Remote sensing techniques in benthic ecosystems involve more considerations than standard remote sensing for terrestrial environments, largely due to the varying influence of the water column (Traganos & Reinartz, 2018a). To derive quantitative data on optically shallow waters, it is necessary to correct atmospheric, air-water interface, and water column interferences (Ibid). Formula 1 explains the path of light in remote sensing in water.

$$L_u = L_a + L_r + L_w \quad (1)$$

In detail, the sensor captures three different types of radiance: atmospheric contribution, water-leaving radiance, and surface-reflected radiance. The atmospheric contribution is known as L_a and comes from solar radiance scattered by gasses and aerosols in the atmosphere. When light hits the water's surface, some portion of light penetrates the water column in the face of underwater seagrass bed communities, and some of it gets refracted. The penetrated portion is also altered by the suspended sediments and phytoplankton in the water column (Veettil et al., 2020). These effects intensify with increasing water depth and turbidity, causing a notable exponential decline in light intensity (Simpson et al., 2022). Some return signal is scattered upward, leaving the sea surface in the sensor direction, resulting in water-leaving reflectance L_w .

Additionally, surface-reflected radiance L_r occurs when light directly reflects toward the sensor due to the alignment between the sun's position and the sensor's viewing angle of the water. This effect might be limited to specific viewing angles involving waves or could extend widely across substantial sections of an image (Kay et al., 2009). Consequently, only L_w is informative about the water column, the seafloor, and optically shallow water. In essence, L_u is the sum of the aforementioned radiance.

The ability to detect seagrass in satellite images relies on spectral resolution, which is determined by the spectral reflectance of seagrasses and the degree to which the water column affects this radiation (Bai et al., 2023). This absorption primarily occurs in the visible (400-700 nm) and infrared radiation (1000-2000 nm) ranges (Veettil et al., 2020). The visible spectral range, such as blue, green, and red bands, penetrates deeper into the water column (Traganos & Reinartz, 2018b). However, the red band is entirely absorbed at a depth of approximately three meters, and it is used to compensate to a degree for under or overcorrection of atmospheric interference (Ibid) (Li et al., 2020). Additionally, the ultra-blue band has greater penetration but scatters easily (Ibid). Since spectral differences between seagrass species are often subtle, and epiphytic plants may interfere with the

2. Theory and State of the Art

spectral signature, differentiating between seafloor habitats and seagrass species presents a challenge (Simpson et al., 2022) (Busch et al., 2016).

As light travels deeper into the water column, it becomes increasingly absorbed and scattered, resulting in a significant decline in distinguishing between different seagrass communities using optical remote sensing data (Veetil et al., 2020). Wavelengths beyond 680 nm undergo significant attenuation as they penetrate the water column, being easily absorbed and attenuated, thus unsuitable for seagrass identification (Ibid).

Depth is also a limiting factor, as all radiation is absorbed before it can reach the seabed, which means no bottom signal is returned to the sensor. Therefore remote sensing is typically only effective in the top ten meters of shallow systems due to light attenuation affecting the retrieval of benthic information (Ibid). These limitations pose challenges for remote sensing in coastal ecosystems, as atmospheric interference, water turbidity, and sun glint reflectance can all contribute to poor image quality and inaccurate estimations if not considered in the image pre-processing phase (Ibid).

The accuracy of monitoring seagrass beds with multispectral remote sensing is significantly influenced by the spatial resolution. As the spatial resolution of an image increases, more detailed spatial information is provided (Bai et al., 2023). Free images from satellites like Sentinel 2, which have a 10-meter resolution, have shown promising results in accounting for this ecosystem (Traganos & Reinartz, 2018a). Satellites with smaller resolution, like Landsat, have also been utilized for this purpose, leveraging their high temporal resolution to conduct more extensive time-scale studies (Li et al., 2020). More recently, smaller spatial resolutions, such as the PlanetScope images, have been introduced, further enhancing the ability of these tools to measure seagrass coverage (Lee et al., 2023).

Effectively measuring the complex and often non-linear processes of seagrass carbon sequestration through remote signals presents challenges (Simpson et al., 2022). Thus, to accurately measure the carbon stocks in seagrass through remote sensing, it is necessary to understand the biophysical processes involved in seagrass carbon sequestration. This requires using proxies to estimate carbon content that considers the unique natural characteristics of the ecosystem (Ibid) (Hein, 2014). By modeling these natural processes and combining the resulting data with satellite imagery and environmental observations, we can obtain a more comprehensive understanding of the dynamics of biophysical parameters in seagrass ecosystems.

2.2.2. *Biophysical models for carbon estimation in seagrass*

The System of Environmental Ecosystem Accounting (SEEA-EA) is an innovative statistical framework developed by the United Nations for measuring habitat services and linking them to human and economic activities (Ibid). This approach leverages spatially explicit data to delineate ecosystems and identify health indicators, intending to inform policy formulation and advance the achievement of the Sustainable Development Goals (United Nations, 2022).

The process of modeling carbon storage and sequestration in seagrass ecosystems involves a detailed and spatially explicit approach that recreates natural processes and components (United Nations, 2022). As defined by SEEA-EA, biophysical modeling is a quantitative estimation of complex processes that are not easily observed directly. The approach also utilizes a tiered system, similar to the one proposed by the IPCC for carbon accounting. Tier 1 relies on globally available data, while Tier 2 requires national datasets that require customization and validation. Finally, Tier 3 is based on local data (IPCC, 2023).

In this research, we employed the InVEST Coastal Blue Carbon (CBC) model to assess the various pressures contributing to carbon emissions and to estimate the potential carbon accumulation over time in seagrass vegetation. The objective was identifying locations with net carbon gains or losses over time. This model, developed by Stanford University and the Natural Capital Project, is an open-source tool that enables reproducibility and transferability across different regions. It factors in carbon storage across four pools- AGB, BGB, sediment, and standing dead carbon- and calculates the total carbon stored by summing up the carbon in these pools.

The Coastal Blue Carbon Modeling approach simplifies the carbon cycle calculation by determining carbon stocks for a given year t and combining them with the net carbon sequestration of the previous year $t - 1$, for each pool p (Formula 3). Alternatively, it could use the starting stock values from the biophysical table $S_{p,t_{baseline}}$. This approach assumes that carbon accumulates linearly over time.

2. Theory and State of the Art

$$S_{p,t} = \begin{cases} S_{p,t-1} + N_{p,t} & \text{if } t > t_{baseline} \\ S_{p,t_{baseline}} & \text{if } t = t_{baseline} \end{cases}$$

Formula 3.

The model utilizes a spatially explicit approach, which combines EO with biophysical parameters to calculate the carbon content of seagrass ecosystems. The input to execute the CBC model includes maps of coastal ecosystems, the amount of carbon stored in tonnes/ha for each carbon pool (biomass, soil, and litter), the annual rate of carbon accumulation in the biomass and soil, the half-life of carbon in the biomass and soil pools, and the level of disturbance suffered by the ecosystem.

The Carbon Sequestration and Storage is another model within InVEST using maps of land use and stocks in the four carbon pools to estimate carbon currently stored in a landscape and the amount of carbon sequestered over time. This model assumes a linear change in carbon sequestration over time. This model was also used to determine the carbon dynamic on seagrass in the area.

3. Study area

The Caribbean Sea region has a high amount of seagrass compared to its coastline, making it one of the regions with the highest seagrass extents (McKenzie et al., 2020). Given the diverse array of environmental factors shaping the distribution of seagrass species, they are valuable bio-indicators for monitoring climate change and ecosystems' overall health (Veettil et al., 2020) (McKenzie et al., 2020).

The study area is located on the west coast of Belize, the Belize Barrier Reef Reserve System (BBRRS) part of the Mesoamerican Barrier Reef System (Figure 1). The Mesoamerican Barrier Reef System is the most extensive barrier reef in the Western Hemisphere, as reported by the World Wide Fund for Nature (2019). The BBRRS is renowned globally for its diverse reef structures, thriving coral growth, and large seagrass beds (WWF, 2019). It is considered a prime example of the evolution of reef systems (Gibson et al., 2004), designated as a UNESCO (2023) World Heritage site. Additionally, the research area represents a significant distribution zone for seagrass beds within the Caribbean Sea.

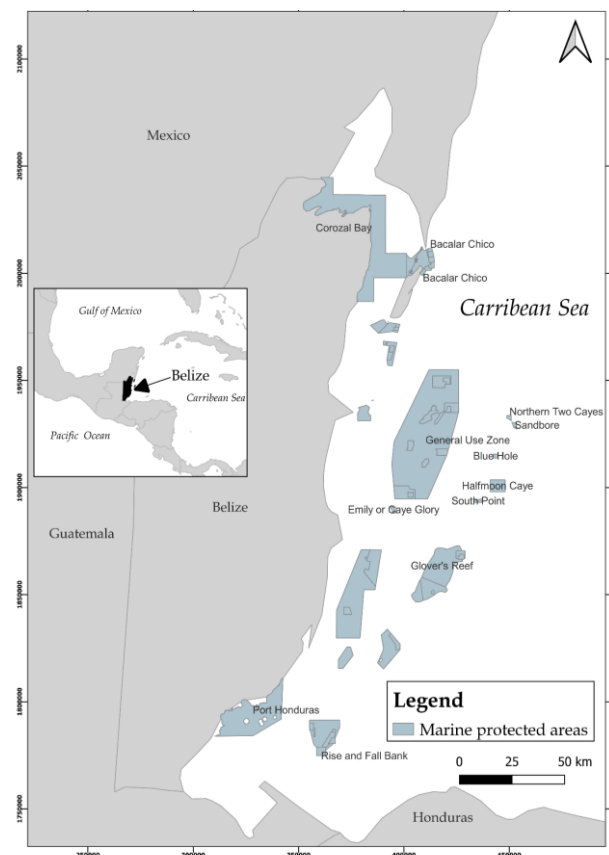


Figure 1. Overview of the Belize Barrier Reef Reserve System and Atolls systems. True-color Sentinel-2 imagery. Marine protected areas (MPAs) are displayed in orange, and UNESCO (2023) World Heritage Sites are in green. Three atolls (Turneffe, Lighthouse, and Glover's Reefs) are outside the BBRRS (Gibson et al., 2004).

3. Study area

The Economic Exclusive Zones (EEZ) of Belize spans 34424 sq km, featuring an extensive coastline of 368 km. This water area boasts a diverse bathymetry ranging from 10 to 30 m in depth. It is home to various lagoons, atolls such as Turneffe Atoll, Lighthouse Reef Atoll, and Glover's Reef Atoll and islands (Gibson et al., 2004). Belize's EEZ includes 15 marine protected areas (MPAs), which utilize innovative methods for incorporating ecosystem services into stakeholder-led planning and decision-making processes (Verutes et al., 2017).

In the region, seagrass beds are mainly found in shallow nearshore waters of up to 1 meter, associated with marine brackish-protected bays and estuaries or reef systems (WWF, 2022) (Tussenbroek et al., 2014). Turtle grass is the primary species prevalent along the coasts throughout the region (Wabnitz et al., 2008). *Halodule wrightii* and *Syringodium filiforme* species exist in lesser abundance (Gallegos et al., 1994) (Carpenter et al., 2022).

The coastal and marine ecosystems in Belize are critical to the livelihoods of over 60% of its population. According to Verutes et al. (2017), reef-based tourism, fisheries, and scientific research contribute around 15% of Belize's gross domestic product annually. Despite the economic benefits of these activities, they pose significant risks to the marine and coastal ecosystems that sustain them. As highlighted by Gibson et al. (2004), activities such as coastal development, aquaculture practices, and dredging can cause significant damage to benthic habitats in the region. In addition, agricultural and urban runoff pollutants are major challenges that threaten the health of the Belizean seagrass (Hejnowicz et al., 2015) (Carlson et al., 2021).

4. Materials and Methods

The study utilizes biophysical modeling to examine organic carbon in seagrasses, with a focus on forecasting carbon abundance in the Caribbean region through a pilot study in Belize. The research comprises two phases. In the first stage, high-resolution remote sensing data is employed to identify the presence of seagrass in Belize's Economic Exclusive Zone, and we analyze changes in this ecosystem from 2016 to 2022 by comparing two sets of composites with different spatial resolutions. In the second part, we model the changes in carbon content on seagrass using the Coastal Blue Carbon tool, which utilizes spatial explicit information. We incorporate the results from the first step into this model, using literature review data on biomass, soil carbon, accumulation rates, and net sequestration. Figure 2 shows the utilized workflow.

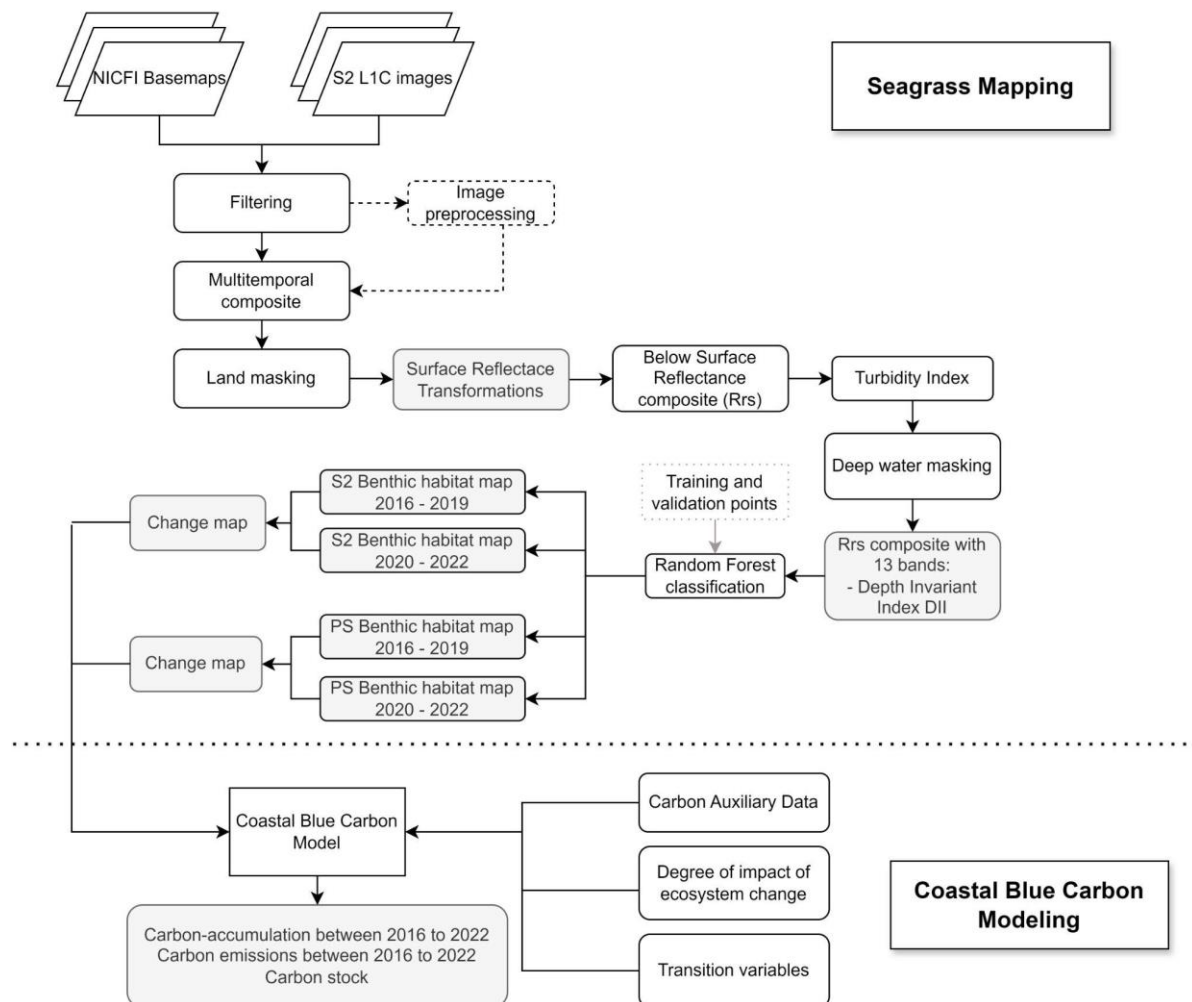


Figure 2. Process of generating a classification of benthic habitat maps from a single image composite for each period.

4. Materials and Methods

4.1. Seagrass Mapping

4.1.1. Data sources

We used two satellite data sources to obtain a better understanding of the distribution of benthic habitats in the region.

The first set of images was the Harmonized Sentinel-2 MSI: MultiSpectral Instrument, Level-1C image collection available on Google Earth Engine (GEE). The Sentinel 2 Level 1C (S2 L1C) product includes radiometric and geometric corrections, orthorectification, and spatial registration on a global reference system with sub-pixel accuracy. It offers thirteen spectral bands ranging from range from the Visible (VNIR) and Near Infra-Red (NIR) to the Short Wave Infra-Red (SWIR), with four bands at 10 m, six bands at 20 m and three at 60 m spatial resolution (SUHET, 2014).

The research also utilized PlanetScope Surface Reflectance Mosaics, consisting of analysis-ready data that have been corrected to minimize the effects of atmosphere and sensor characteristics. They have a spatial resolution of 4.77m with a spectral resolution of four bands, three visuals (Blue, Red, Green) and one Near-Infrared (Planet, 2022).

To produce the classification maps, we integrated visual points and reference points from the official maps of the Ministry of Blue Economy and Civil Aviation of Belize. An unsupervised classification was conducted on the PS and S2 composites, resulting in five classes for habitat mapping. To achieve considerable mapping accuracy, we identified 5 classes - seagrass, coral, sand, rubble, and deep water - to select the most representative ecosystem in the area. The points were examined manually to verify that they belonged to their respective classes. Additionally, we cross-checked our results with the Allan Coral Atlas benthic maps in the area, the UNEP-WCMC (2021, 2024) Global Distribution of Coral Reefs v.4 dataset and PS single scenes. A total of 510 sand and rubble points were drawn to represent marine substrates.

Following the necessary data standardization and conversion procedures, we employ an averaging technique to derive single points for the classification map. These points indicate the presence of various benthic habitats, including seagrass and coral, and sediments, such as sand and rubble. Given the intricacy of the region, we ensure that deep waters are included in the classification process.

For the validation, we collected data from two benthic maps, one from 2016 and the other from 2020, by randomly selecting points. A reprojection and resolution reduction was done in order to match the resolution of our composites. To guarantee the precision of the results, we first created an intersection map that reflected the habitats present in both time

4. Materials and Methods

frame maps. Refer to Table 1 for the total of training points by source and snapshots of each class and Figure 3 for their spatial distribution.

| Source | Dates | Number of points |
|------------------------------|-------------|------------------|
| Manual visualization | 2016 - 2019 | 1590 |
| Official Belize Benthic Maps | 2016 - 2020 | 300 |
| Total | | 1890 |

Table 1. Source of training points

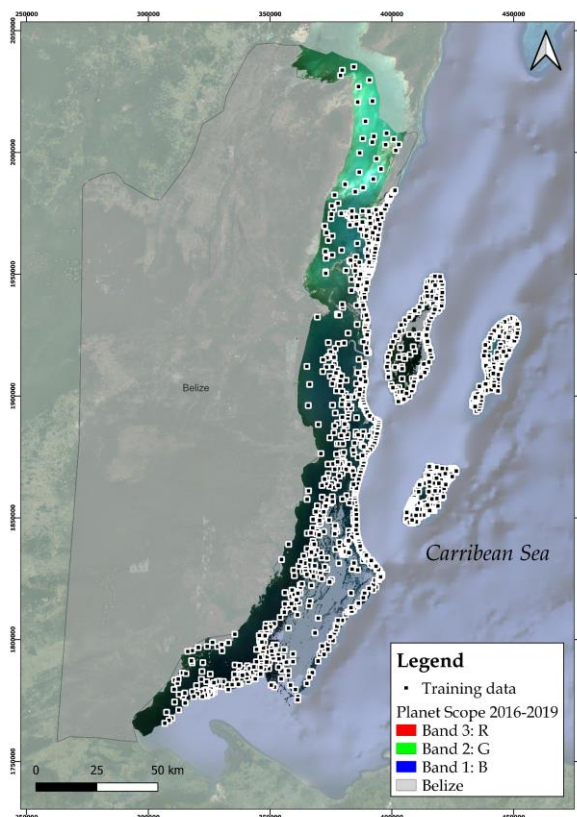


Figure 3. Training TD data distribution throughout the AOI.

4.1.2. Multi-temporal composite

As part of the study, two sets of composites were tailored to align with the defined periods of January 2016 to December 2020 and January 2021 to December 2022. These periods span three and four years of observations, respectively. A multi-year timeframe was deemed necessary to minimize the impact of atmospheric cloud interference and to achieve sufficient data coverage. Previous studies have shown that using 3-year periods

4. Materials and Methods

for mosaics can reduce cloud cover, haze, and sunlight interference in water mosaics (Schill et al., 2021) (Blume et al., 2023).

The first set corresponds to two four-band (blue, green, red, near-infrared) surface reflectance composites from PS Basemaps 37 mosaics. The second pair of mosaics were created with S2 L1C images. These composites include the 'B1', 'B2', 'B3', 'B4', 'B5', 'B8', 'B8A', and 'B11' bands. In total, 2263 S2 images and 38 PS quads were selected (see Table 2 for composite details).

| Dates | Image collection source | Number of PS quads / S2 scenes images |
|------------------------------|--|---------------------------------------|
| January 2016 - December 2019 | NICFI Semestral Basemaps S2-L1C | 8 1229 |
| January 2020 - December 2022 | NICFI Semestral Basemaps NICFI Monthly Basemaps S2-L1C | 1 29 1007 |

Table 2. Composite details. Number of single scenes for S2-L1C and quads for NICFI Basemaps utilized for constructing the composite image.

Several pre-processing techniques were required to identify the benthic in the satellite images. The pre-processing workflow for the images was conducted in GEE to accommodate the data's computationally demanding nature. Adjustments were made to the cloud-native S2 L1C image pre-processing workflow following previous work done by Blume et al., 2023 and Traganos et al, 2022 and the NICFI Basemaps processing workflow done by Lee et al., 2023.

In our methodology, we endeavored to adhere to a compatible approach in generating composites for both datasets. However, we implemented distinct procedures tailored to the specific attributes of each image set to ensure alignment with the unique characteristics of the data. The specific research workflow is shown in Figure 1.

First, an environmental noise correction was performed to derive a multitemporal composite. The S2 images underwent preprocessing, selecting images containing less than 10% cloud cover being used. Additionally, a cloud mask was applied using the QA60 band and a bitmask band with cloud mask information, and we rescaled the TOA values. On the contrary, as the NICFI Basemaps are generated using the best available pixels for the site, no further environmental noise filtering was necessary.

4. Materials and Methods

In order to create a single multi-temporal composite per image source and per timeframe, we calculated different percentiles to determine the ideal fit for the composites. We selected the 20th percentile as the best statistical metric for reducing the impact of sunglint, turbidity, clouds, and haze in the area (Donchyts et al., 2016). This step was taken based on its superior performance, as described in the study by Traganos et al. (2022). Because of the minimal tidal fluctuations in Belize, typically around 0.3 meters, the tidal stage was not considered (Gischler, 2011).

We used the combined Otsu-based method for bimodal thresholding and the Canny edge filter method to differentiate land from water in the pair of images (Donchyts et al., 2016). This involved setting an optimal threshold to maximize inter-class variance based on the distribution of pixel values observed in the Normalized Difference Water Index (NDWI) of each composite (Equation 1) for the PS composite and the Modified Normalised Difference Water Index (mDWI) for the S2 L1C image (Equation 2). All histograms used for the Otsu-based maskings achieved bi-modal distributions.

$$NDWI = Green - NIR / Green + NIR$$

Equation 1.

$$MNDWI = Green - SWIR1 / SWIR1$$

Equation 2.

We performed an atmospheric correction to the composite after masking out terrestrial regions. The resultant image represents the normalized reflectance above the water surface, denoted as R_{rho} (Equation 3). The composite of the normalized water-leaving reflectance (R_{hown}) was adjusted to account for the differences in the optical path between the air and water column. To make this correction, we obtained the Below-surface remote sensing reflectance $R_{rs}(\lambda)$, which describes the ratio of the radiance leaving the water to the radiance coming down immediately above the water surface (Traganos & Reinartz, 2018a)

$$R_{rs} = R_{hown} / \pi$$

Equation 3

A turbidity index was implemented to mitigate the impact of light attenuation in turbid coastal waters. The index is rooted in a linear model employing distinct spectral profiles to

4. Materials and Methods

represent each class (Pertiwi et al., 2021). In order to train the model, a set of 160 training data points TD, along with sampled reflectance values, were used, while 40 validation points VD were employed to ensure accuracy (Appendix A). It was confirmed through a visual analysis that the same TD and VD used in both NICFI mosaics correspond accurately to areas with and without turbidity in both images. The same process was followed with the S2 L1C image, using the same number of VD and TD points.

Figure 4 below shows the results of the Random Forest classification maps. The classification algorithm that performed the best was a Random Forest. All the classification maps were created using 1590 points for training and 300 for validation, 80% corresponding to training (TP) and 20% to validation points (VP).

A Hue-Saturation-Value (HSV) mask was created to exclude deep water pixels in the images. This approach proved effective in addressing the band limitations of PlanetScope, as noted by Lee et al. in 2023. Additionally, the N band was kept for the downstream feature development step instead of being eliminated by the conventional atmospheric correction (Lee et al., 2023).

We applied a deep water mask using Satellite-Derived Bathymetry (SDB) to remove the remaining deep water pixels from the map. The conditions for this mask were set to include only areas at least 10 meters deep, considering the mapping efforts of the Allen Coral Atlas in the Caribbean (Schill et al., 2021). Most of the seagrass beds in the study area are distributed between 0.3 to 10 m below the water's surface thus we used this depth to refine the categorization process.

A recovery mask was applied for all previous steps to conserve pixels on Turneffe Atoll, Lighthouse Reef Atoll, and Glover's Reef Atoll. Prior research has consistently undervalued the prevalence of seagrass within this lagoon ecosystem (Gaston et al., 2009) (Short et al., 2006) (Carpenter et al., 2022); therefore, we incorporated these areas into our composite analysis to address this oversight.

Using a log-linear transformed linear model, two depth-invariant bands were created from the red, green, and blue bands (Lyzenga et al., 2006). Further bands were generated after completing the necessary steps to facilitate future benthic habitat mapping. Consequently, an ultimate composite comprising 18 bands was produced for S2 L1C. The computed NICFI resulted in a 5-meter spatial resolution with 13 bands. Refer to Table 3 for details of the S2-L1C and PS composites.

4. Materials and Methods

| | Rrs Sentinel-2 L1C composite | Rrs PS composite |
|--------------------|--|--|
| Spatial Resolution | 10 m | 5 m |
| Bands | Coastal aerosol Blue Green Red Vegetation red edge NIR Vegetation red edge SWIR Coastal aerosol - Blue Blue-Green Coastal aerosol - Green Hue Saturation Value NDWI mDWI Blue-Green Green-Red Blue-Red Slope Depth | Blue Green Red NIR Hue Saturation Value NDWI Blue-Green Green-Red Blue-Red Slope Depth |

Table 3. Rrs Sentinel-2 L1C and NICFI composites characteristics

4.1.2.1. Mapping method of seagrass bed distribution

The classification aimed to differentiate the benthic ecosystems in shallow Belizean waters based on their spectral classes that represent the unique patterns of each ecosystem. A Random Forest RF model was trained with 50 trees in GEE, identifying five distinct classes: seagrass, coral, sand, rubble, and deep water. The selected benthic categories were simplified into broader classes to ensure accurate classification across the created composites. For instance, the dense and sparse seagrass categories were merged into one class to maintain consistency across the mosaics while accounting for resolution differences. Furthermore, this study made no distinction between seagrass classes.

4. Materials and Methods

The seagrass extent maps were thoroughly evaluated using the data sets generated in this and prior studies (Schill et al., 2021) (Busch et al., 2016) (F. T. Short et al., 2006) (Carpenter et al., 2022). These previous studies were selected due to their similar temporal and spatial scales and areas intersecting the 2016-2019 and 2020-2022 maps.

Following the initial training phase, we analyzed the variable importance of each image band in relation to the model's accuracy. Based on this assessment, we identified the ten most crucial features for each image and then we proceeded to a secondary training phase, enhancing the classification by prioritizing the variables with the highest impact.

The classification outcomes were evaluated by calculating overall user (OA) and producer accuracy (PA) for the RF classification. Furthermore, the high-resolution PlanetScope scenes of the study area were utilized as a reference. The visual assessment was used to determine the correctness of the classification.

4.1.2.2. *Change detection analysis of seagrass extent*

Studying the alteration in the benthic environments is crucial in comprehending the carbon dynamics over time. To achieve this, a change detection analysis was executed, and the variation was determined by computing the difference between two composite epochs, the initial period (2016 - 2019) and the subsequent (2020 - 2022).

First, each set of maps was co-registered in Rstudio to ascertain whether changes were due to the gain or the loss of the ecosystem in the area. The gains and losses of the ecosystems were measured in sq km, alongside the per-pixel analysis indicating increases, stability, or decreases between 2016 and 2022.

4.2. Coastal blue carbon modeling (Biophysical modeling)

4.2.1. *Carbon estimates*

Accurately evaluating the impact of seagrass on sedimentary organic carbon stocks requires a comprehensive assessment of carbon parameters. To accomplish this, we selected various biophysical factors, including biomass, soil carbon data, accumulation rates at a given year, and net sequestration. As public data on seagrass carbon health at a national or local scale was not accessible, we reviewed data from previous studies to inform our analysis.

The search method used to identify carbon values associated with seagrasses in the Caribbean. It utilized Spanish and English keywords to ensure a comprehensive search,

4. Materials and Methods

including terms like "carbon," "seagrass," "benthic habitat," and "seagrass meadow" to target the ecological and carbon-related aspects of seagrass environments. The search was geographically focused on "the Caribbean," "Caribbean countries," and specifically "Belize" to provide a broad yet focused selection of studies within the region. To gain a thorough understanding of carbon storage and processes, the search criteria included terms such as "biomass," "above-ground biomass," "below-ground biomass," "litter," "sediment," and a focus on "carbon accumulation," "organic matter," and "bulk density", "soil", "sediment", "carbon sequestration", and "carbon stock". The research also included "*Thalassia testudinum*" as this is the principal species found in the region.

For calculating the parameters included in the biophysical table, we utilized specific data provided about carbon in seagrasses (Table 4). The initial carbon stock in the soil, represented as Soil-initial in tonnes per hectare, was obtained from the study by Herrera-Silveira et. al., 2020 conducted in Mexico. Due to the proximity, it was taken into account for Belize, which indicated that these meadows store an average of 241 ± 118 Mg Corg ha⁻¹ in the top 1-meter thick soil layer. The calculation for the initial biomass in seagrass ecosystems was based on data provided regarding the average above-ground and below-ground biomass. Data on accumulation was taken from Fu et. al., 2023 in a study developed in the Caribbean, Bahamas and soil from research from Duarte et. al., 2016 using the estimation Stankovic, 2021 made for the region. Moreover, data about half-life and disturbance was taken from the user guide recommendation for seagrasses from Murray et al, 2011 and Montero-Hidalgo et. al., 2023.

4. Materials and Methods

| Parameter | Value | Tier | Source |
|--|-------|------|---|
| Biomass-initial (tonnes/ha) | 1.6 | 1 | Lovelock et. al., 2017 |
| Soil-initial (tonnes/ha) | 52.32 | 2 | Herrera-Silveira et. al., 2020 |
| Litter-initial (tonnes/ha) | NA | NA | NA |
| Biomass-yearly-accumulation (tonnes/ha year) | 2.13 | 1 | Fu et. al., 2023 Duarte, C. M., N. Marba, et al., 2010 |
| Soil-yearly-accumulation (tonnes/ha year) | 1.60 | 2 | Duarte et. al., 2016 Stankovic, 2021 |
| Biomass-half-life (year) | 0.27 | 1 | Murray et al., 2011 |
| Biomass-high-impact-disturb (ratio) | 1.00 | 1 | Murray et al, 2011 Montero-Hidalgo et. al., 2023 |
| Soil-half-life (year) | 1.00 | 1 | Murray et al, 2011 |
| Soil-high-impact-disturb (ratio) | 0.50 | 1 | Murray et al, 2011 Montero-Hidalgo et. al., 2023 |

Table 4. Data Sources for Estimating Metrics in the InVEST Blue Carbon Biophysical Model

Moreover, this study calculates carbon sequestration and storage using the Carbon Storage and Sequestration in InVEST. For this purpose, information on carbon content on the four pools for seagrass was described (Table 5). These data were acquired by literature review.

| lucode | LULC_Name | C_above | C_below | C_soil | C_dead |
|--------|------------|---------|---------|--------|--------|
| 1 | sand | 0 | 0 | 0 | 1 |
| 2 | seagrass | 0.8 | 1.8 | 140 | 0 |
| 3 | rubble | 0 | 0 | 0 | 0 |
| 4 | coral | 0 | 0 | 0 | 0 |
| 5 | deep water | 0 | 0 | 0 | 5 |

Table 5. Data Sources for Carbon Pools for Estimating Metrics in the InVEST Carbon Storage and Sequestration Model

4. Materials and Methods

4.2.2. *Carbon fluctuations*

The model contains a transition table that provides information about the intensity of ecosystem changes. The changes are defined as an accumulation of low-impact disturbances (e.g., sand to seagrass) or high-impact disturbances (e.g., seagrass to sand). The transitions table was thoroughly completed, taking into account the various possibilities of change between ecosystems. For example, we designated changes from SG to SD as "disturbance," while the opposite was labeled as "accumulation" (see Appendix).

4.2.3. *Application of InVEST for Coastal Blue Carbon Biophysical Modeling*

Initially, spatially explicit maps were calculated and seamlessly integrated into the model for accurate results. In this step, we utilized the full benthic classification in order to gain a comprehensive understanding of the changes occurring in the region.

After several iterations of the model, we obtained the final output comprising of six detailed maps that highlighted carbon accumulation and emission from 2016 to 2022, carbon stock at 2016, and the total net carbon sequestration.

5. Results

In this section, we analyze the outcomes of the analysis outlined in the previous section. Initially, we focus on the results derived from seagrass maps and identify the change detected in two distinct periods - firstly, one composite with images from 2016 to 2019 and one composite from 2020 to 2022 to identify the change in seagrass levels within the coastal area of Belize. Next, the carbon accumulation with the seagrass is calculated to identify the total net carbon sequestration - this was done using the InVEST CBC model and Carbon Sequestration and Storage model. The model performance was accessed to understand the accuracy of the results. Lastly, we undertook a comparative analysis using different satellite images, PS with a resolution of 5m and S2 with a resolution of 10m, on the performance of the model and its ability to calculate carbon acquisition.

5.1. Seagrass extent and change detection in the distribution of seagrass

This section explores the creation of comprehensive maps of benthic habitats in Belize, with a specific emphasis on seagrass. This was achieved by developing a multi-temporal below-surface remote sensing reflectance composite from 2016 to 2019 and one composite from 2020 to 2022. The end result was two classification maps using PS images and two classification maps using S2 data.

The classification was done within the marine environments of Belize. There five classes that were mapped, these were:

1. Sand
2. Seagrass
3. Rubble
4. Coral

5. Results

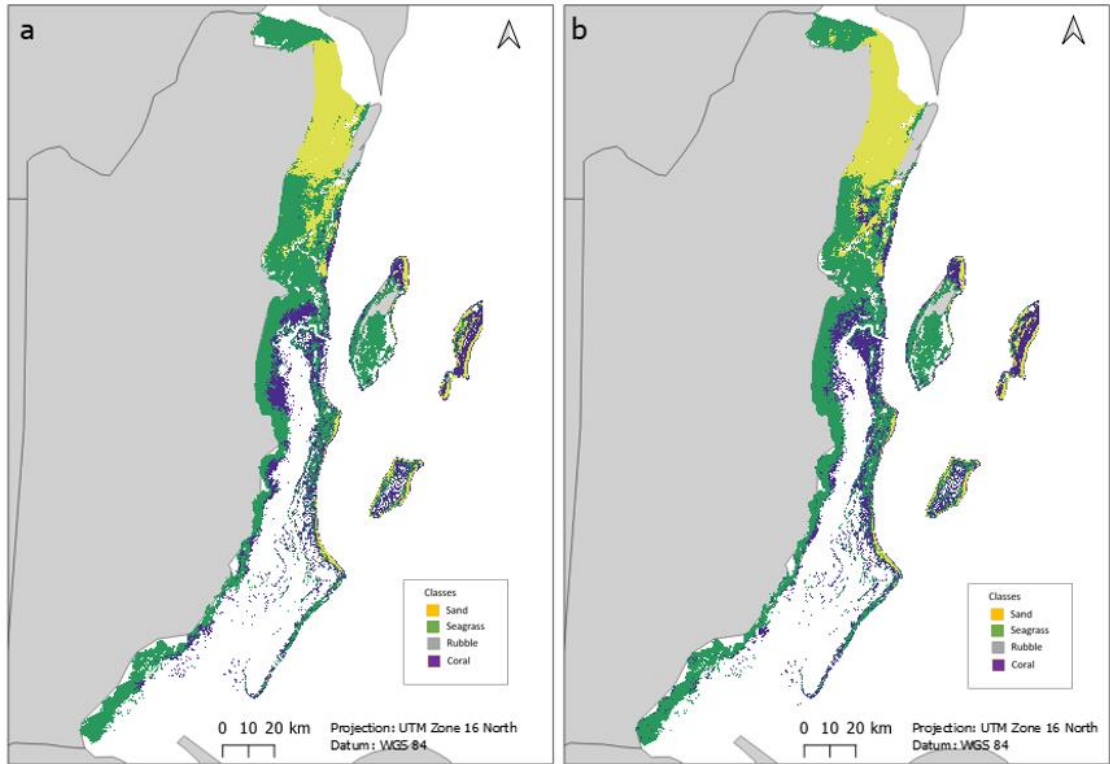


Figure 4. Classification results of all classes in the Belizean Marine environment using the random forest algorithm on the PlanetScope composites

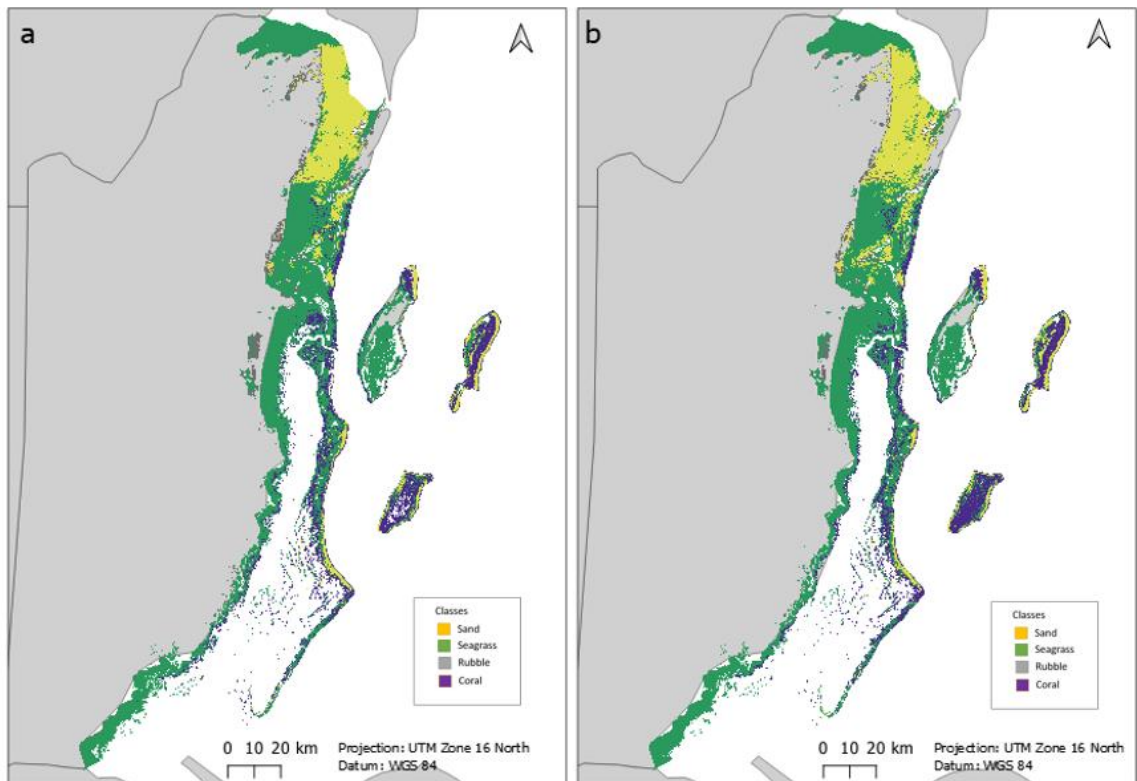


Figure 5. Classification results of all classes in the Belizean Marine environment using the random forest algorithm on the Sentinel-2 composites

5. Results

The results in table 5 display the extent of seagrass identified. The S2 images were able to identify 409.6 sq km more in the periods of 2016 - 2019 than PS images and in the period of 2020 - 2022 S2 images identified 466.7 sq km. S2 images used were able to classify a larger area extent of seagrass than PS images.

| | PS 2016 - 2019 | PS 2020 - 2020 | S2 2016 - 2019 | S2 2020 - 2020 |
|------------------|----------------|----------------|----------------|----------------|
| Seagrass (sq km) | 2912.50 | 2830.12 | 3322.1 | 3296.82 |

Table 6. Seagrass Coverage Area in Square Kilometers Determined for Each Image Composite

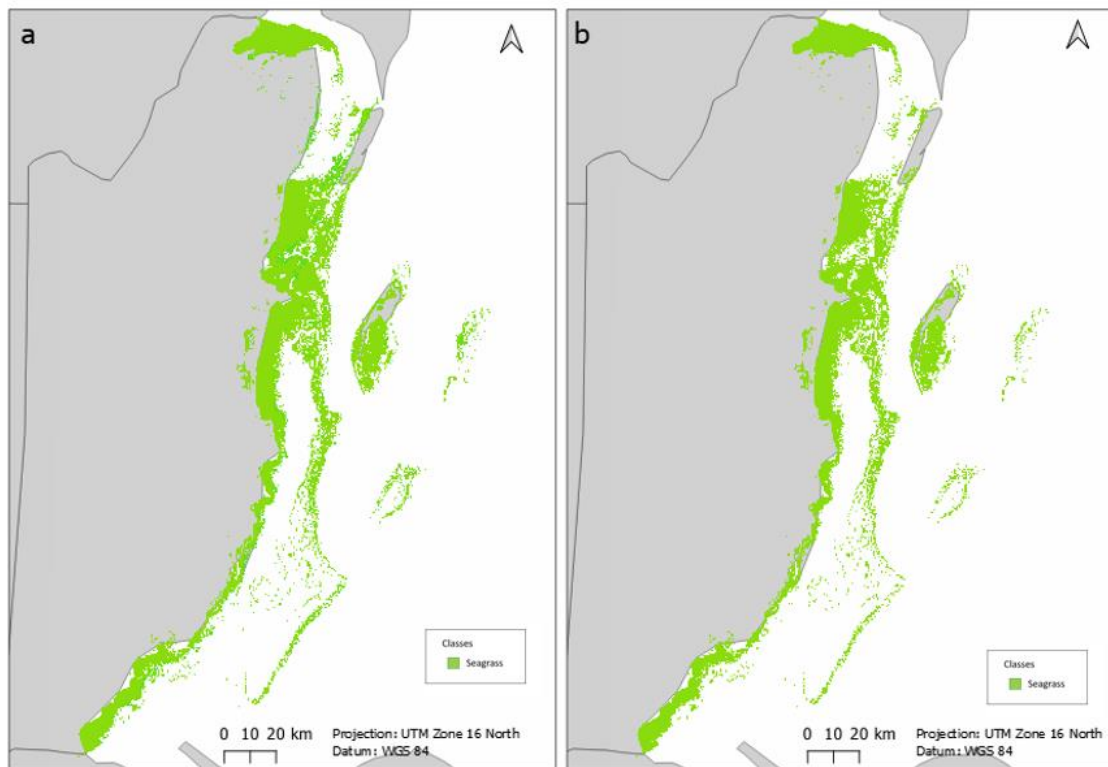


Figure 6. Seagrass extension in the Belizean Marine environment using the random forest algorithm on the Sentinel-2 composites.

5. Results

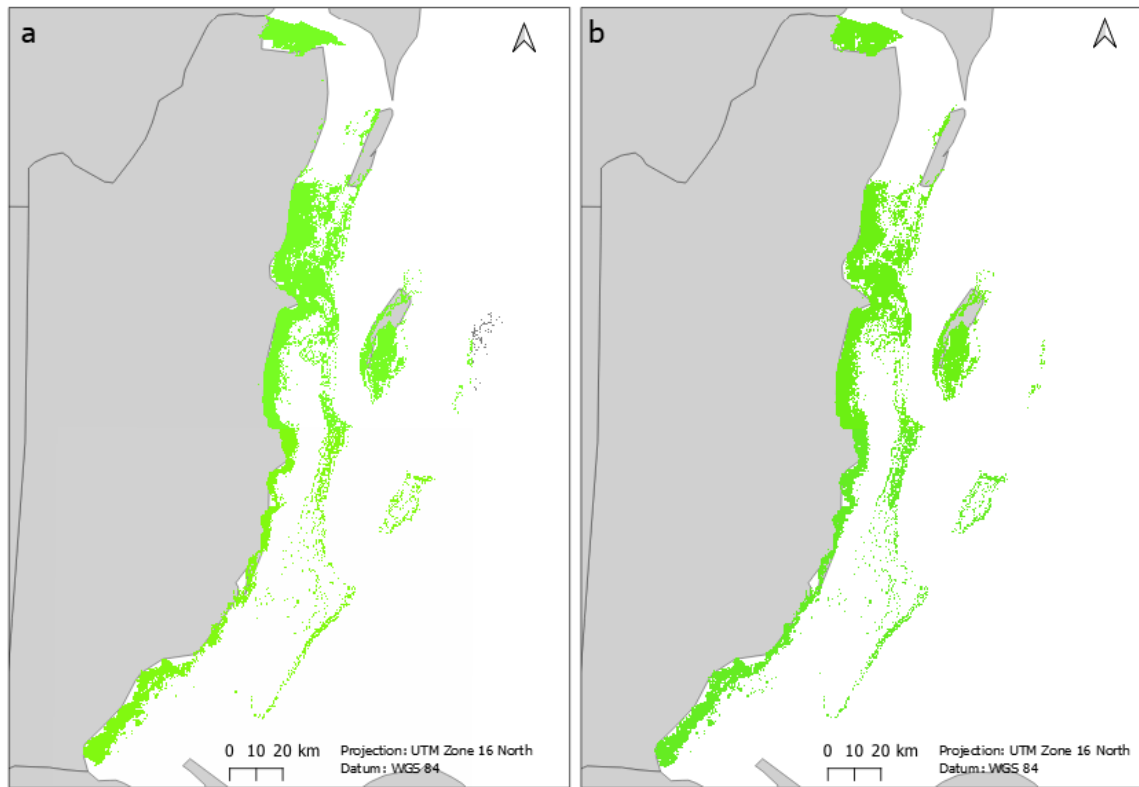


Figure 7. Seagrass extension in the Belizean Marine environment using the random forest algorithm on the PlanetScope composites.

The classification results obtained through the random forest algorithm for the Belizean Marine environment are summarized in Table 6. Seagrass emerges as the predominant class across all datasets, underscoring its paramount importance and the imperative for its preservation. The extent of seagrass coverage is consistently notable, indicating the critical need for its comprehensive understanding and conservation efforts.

| | Coverage by sand(sq km) | Coverage by seagrass(sq km) | Coverage by coral(sq km) | Coverage by rubble(sq km) | Total area(sq km) |
|-----------------------|-------------------------|-----------------------------|--------------------------|---------------------------|-------------------|
| PS 2016 - 2019 | 1175.14 | 2912.5 | 1029.56 | 100.02 | 5217.22 |
| PS 2020 - 2022 | 1244.95 | 2830.12 | 1096.8 | 124.37 | 5296.24 |
| S2 2016 - 2019 | 1021.03 | 3322.1 | 871.51 | 372.61 | 5587.25 |
| S2 2020 - 2022 | 1121.21 | 3296.82 | 862.65 | 309.1 | 5589.78 |

Table 7. Classification results of all classes in the Belizean Marine environment using the random forest algorithm

5. Results

During the period from PS 2016 to 2019, the coverage of seagrass stood at 2912.5 sq km, accounting for the largest proportion of the total area assessed at 5217.22 sq km. Subsequently, during PS 2020 to 2022, seagrass maintained its dominance, with coverage spanning 2830.12 sq km out of a total area of 5296.24 sq km.

Sand emerges as the second most prevalent class across all datasets, followed by coral and rubble. Notably, while the coverage of sand, coral, and rubble fluctuates slightly across the different periods, seagrass consistently maintains its dominance, emphasizing its ecological significance within the Belizean Marine environment.

To achieve clarity in the imagery and eliminate turbidity, we utilized masking techniques, especially along the coastline. After experimenting with various band combinations, we discovered that setting the threshold at 60 for the B, G, and R bands produced the best results for the NICFI mosaic in 2016 and 2020. For the S2 L1C composites, some bands proved more effective at this threshold. The OA and F1-scores for all four images were similar, ranging from 76 to 79%. However, we observed that the PS composite overpredicted turbidity zones in the northern part of the AOI. Upon a detailed analysis, we concluded that the PS composite was the most precise in removing turbid areas.

The utilization of the random forest algorithm has facilitated a comprehensive mapping of seagrass coverage, shedding light on its spatial distribution and emphasizing the urgency of protective measures. These findings underscore the significance of ongoing research and conservation efforts aimed at preserving the invaluable ecological roles fulfilled by seagrass habitats in marine ecosystems.

5.1.1. Classification accuracy

Table 7 displays the accuracy results obtained from the classification process using the random forest algorithm and provides valuable insights into the reliability and precision of the mapping efforts focused on seagrass within the Belizean Marine environment. These metrics, including Producer Accuracy, User Accuracy, and Overall Accuracy, offer a comprehensive assessment of the classification performance across different datasets and time periods.

5. Results

| | Producer Accuracy | User Accuracy | Overall Accuracy |
|----------------------------------|--------------------------|----------------------|-------------------------|
| PS 2016-2019 Seagrass | 65.16 | 79.9 | 57 |
| S2 2016-2019 Seagrass | 66.68 | 81.59 | 60 |
| PS 2020-2022 Seagrass | 65.54 | 79.4 | 59 |
| S2 2020-2022 Seagrass | 65.71 | 79.44 | 61 |

Table 8. Accuracy of RF model for seagrass maps

For the period spanning PS 2016-2019, the Producer Accuracy for seagrass classification is reported at 65.16%, indicating the proportion of correctly classified seagrass pixels relative to all seagrass pixels present in the dataset. The corresponding User Accuracy stands at 79.9%, representing the proportion of accurately classified seagrass pixels out of all pixels classified as seagrass. The Overall Accuracy for this period is noted at 57, reflecting the overall agreement between the classified results and ground truth data.

Similarly, during the S2 2016-2019 timeframe, the classification accuracy metrics for seagrass exhibit slightly higher values, with Producer Accuracy at 66.68%, User Accuracy at 81.59%, and Overall Accuracy at 0.60. These figures suggest a relatively consistent performance in seagrass classification across different satellite datasets and time intervals.

In the subsequent period of PS 2020-2022 and S2 2020-2022, the accuracy metrics maintain comparability with the earlier periods, with Producer Accuracy for seagrass hovering around 65-66% and User Accuracy ranging from 79.4% to 79.44%. The Overall Accuracy during these periods ranges from 59 to 61, indicating a moderate level of agreement between the classified results and reference data.

The user accuracies for the seagrass class were found to be lower. It is believed that the differences may be attributed to misregistration issues between the image and the validation data. Additionally, the producer accuracy was low, suggesting a potential discrepancy in the classification scheme used.

5. Results

The consistency in accuracy metrics across different time periods and satellite datasets underscores the reliability and robustness of the random forest algorithm in mapping seagrass habitats within the Belizean Marine environment. However, it also highlights potential areas for refinement and improvement in classification techniques to enhance the accuracy and precision of seagrass mapping efforts.

In summary, the accuracy results derived from the classification process using the random forest algorithm are pivotal in the results section of the thesis, providing critical insights into the reliability of seagrass mapping efforts and supporting the estimation of carbon stocks associated with seagrass ecosystems in the Belizean Marine environment.

5.1.2. Change detection in seagrass area extent

In the investigation of the spatial distribution dynamics of seagrasses within Belizean marine environments across the time frames of 2016-2019 and 2020-2022, the change detection analysis using Planet Scope (PS) and Sentinel-2 (S2) satellites reveals significant insights into seagrass gain and loss, and their implications for seagrass carbon stocks.

Table 8 indicates a gain of 359.76 sq km of seagrass coverage and a loss of 473.21 sq km according to the Planet Scope seagrass change map for the period of 2016-2019. Additionally, a substantial portion of 5886.40 sq km of seagrass habitat remained unchanged during this period. Similarly, the S2 seagrass change map shows a gain of 197.76 sq km and a loss of 334.43 sq km of seagrass coverage, with 6532.54 sq km unchanged during the same period.

| | Gain sq km | Lost sq km | No change sq km |
|------------------------|---------------|---------------|--------------------|
| PS seagrass change map | 359.76 | 473.21 | 5886.40 |
| S2 seagrass change map | 197.76 | 334.43 | 6532.54 |

Table 9. Gains and losses for each classification map

The increase in seagrass coverage indicates a potential increase in seagrass biomass, which contributes to the accumulation of carbon stocks within seagrass ecosystems. The observed loss in seagrass coverage highlights areas where seagrass habitats have experienced decline or degradation.

5. Results

In summary, the gain and loss detected in seagrass coverage across the investigated time frames have significant implications for seagrass carbon stocks and ecosystem health (Figure 4).

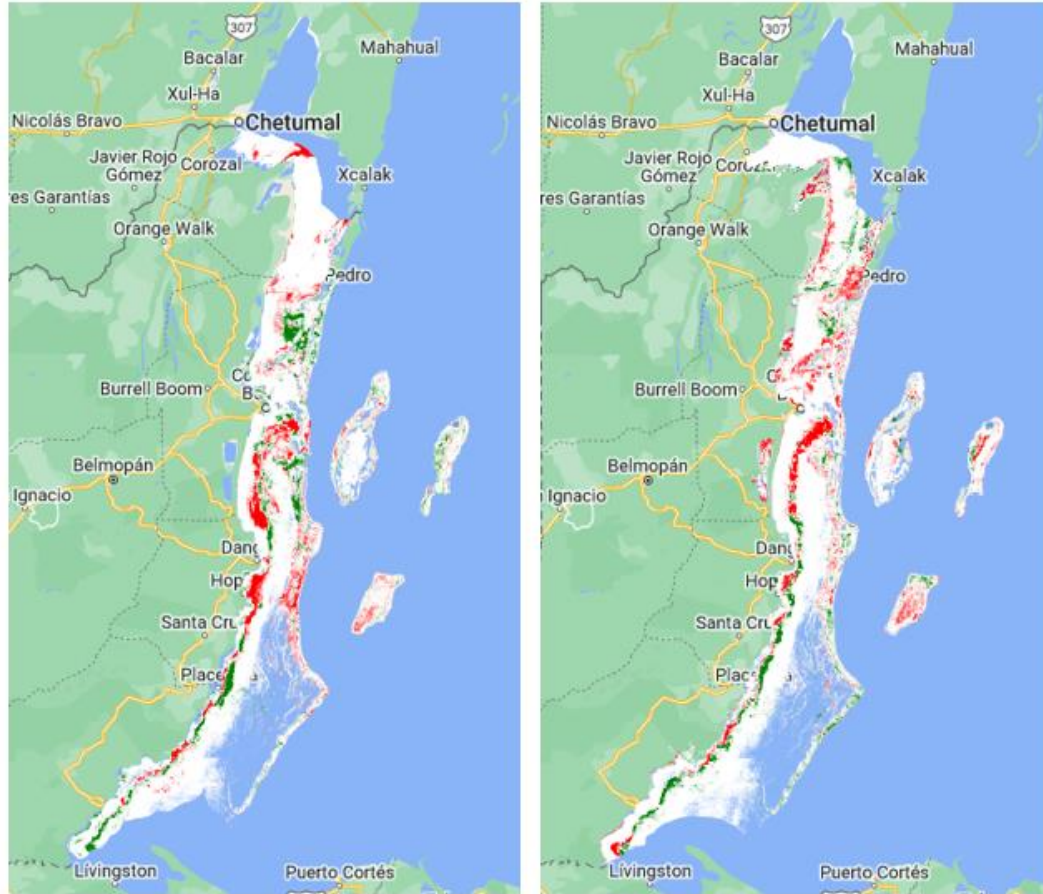


Figure 8. Changes in substrate cover from 2016 – 2022 for seagrass and coral. (=loss, = gain and = no change). Done with PS(a) and S2 (b) maps

5. Results

5.2. Seagrass Blue Carbon Dynamics (Biophysical modeling)

5.2.1. *Estimated carbon stocks with Coastal Blue Carbon Model*

The carbon stock values showed a remarkable increase from 2016 to 2022. Initially, the carbon stock was estimated with a maximum value of 53.92 Mt CO₂e/ha, which more than doubled to 128.52 Mt CO₂e/ha by 2022.

The total net carbon sequestration during this period was significant, with a consistent amount of carbon sequestered according to the provided metrics. This consistency indicates a substantial and continuous carbon uptake process within the ecosystem, contributing to the overall increase in carbon stocks. Additionally, the estimated carbon accumulation during this time period points to a significant amount of carbon added to the ecosystem. The metrics for carbon accumulation align with those of total net carbon sequestration, as shown by the identical values for Estimated Total Net Carbon Sequestration and Estimated Carbon Accumulation between 2016 and 2022 in Appendix.

5.2.2. *Comparison of results of carbon estimations on different scale classifications maps*

These observations for the comparison underscore the importance of utilizing multiple remote sensing sources to capture a more nuanced understanding of carbon dynamics over time.

The PS and S2 datasets both showed a significant increase in carbon stock between 2016 and 2022. This is because the biophysical table used for the model was the same. Specifically, the PS dataset recorded an increase from approximately 6.48 billion to 15.44 billion, while the S2 dataset showed an increase from about 1.89 billion to 4.51 billion. The greater numerical increase in the PS data may be due to its higher spatial resolution, which captured more detailed changes in carbon stock over smaller areas.

Both datasets showed substantial carbon sequestration and accumulation over the period, with the PS dataset reporting a higher total net carbon sequestration sum compared to the S2 dataset. This difference could be attributed to the PS dataset's higher spatial resolution. However, the maximum value for carbon stock and sequestration parameters remained consistent at 74.60 for sequestration and increased similarly for carbon stock in both datasets. This indicates that the maximum potential for carbon sequestration and stock was similar across both satellite observations.

5. Results

The comparison between the PlanetScope (PS) and Sentinel-2 (S2) datasets for biomass and soil carbon accumulation from epoch 1 to epoch 2 highlights distinct trends. For biomass accumulation, both datasets exhibit a decreasing trend; however, the PS dataset starts with a higher average accumulation in 2016 (0.882 Mt CO₂e/ha) that significantly drops by 2022 (0.0198 Mt CO₂e/ha), indicating a substantial reduction.

The S2 dataset, while starting from a similar high in 2010 (0.922 Mt CO₂e/ha), also shows a decline by 2030 (0.050 Mt CO₂e/ha), but not as sharply as the PS dataset. This variation might reflect differences in resolution, influencing the perceived carbon accumulation rates. Similarly, soil carbon accumulation trends decrease in both datasets.

From 2010 to 2030, biomass accumulation shows a notable increase in the maximum value, maintaining at 2.13 in both years, indicating that the potential for biomass carbon sequestration remained consistently high. However, the total sum and mean value decrease from 2010 to 2030, suggesting a decrease in overall biomass accumulation across the studied area. This might indicate that while peak potential for biomass accumulation remains unchanged, the average capacity across the landscape has diminished, possibly due to land use changes, climate factors, or ecosystem management practices.

Soil carbon shows a decrease in both maximum value and overall accumulation from 2010 to 2030. The maximum value remains constant at 1.6, yet the total sum and mean value significantly decrease, pointing towards a reduction in soil carbon storage across the area. This could reflect changes in soil management practices, degradation, or other environmental changes affecting soil carbon dynamics.

6. Discussion

In this section, we will delve into the findings from the analysis of seagrass extent and change detection and the seagrass blue carbon modeling. To facilitate our discussion, we will refer to the first two sections of the ecosystem accounting framework, which focus on assessing the spatial distribution of seagrasses in the area and the capacity of this ecosystem to sequester carbon. We will highlight the performance of the model, limitations, and future directions. Moreover, we will explore how remote sensing and biophysical modeling can be combined to create proxies that further enrich our comprehension of seagrass carbon sequestration.

6.1. Ecosystem extension: Spatial Analysis and Temporal Dynamics of Seagrass Ecosystems

Based on the distribution map of seagrass beds, an analysis was conducted to assess the state and trends of multi-year distribution changes within the study area. Overall, the research indicates that the coverage of seagrass has decreased during the study period. This finding is consistent with previous studies of seagrass mapping conducted in other areas, which also reported a decline in this ecosystem (Gaston et al., 2009).

As part of our initial objective, we aimed to measure seagrass and compare the results between two different time periods to determine whether there were any gains or losses. Our findings revealed that the study area experienced a decrease of 473.21 sq km in seagrass, indicating a net decline of 1.8% in the seagrass ecosystem from epoch 1 to epoch 2, as displayed in Table 8. These results are collaborated by the increase in areas of bare-sand seabed by 2020.

Moreover, the degree of this decrease has varied by region. Both change maps reveal a loss of seagrass in the central north shallow area, which may be related to dredging activities in that region (Figure 9) (Arkema et al., 2014). Additionally, losses close to the coastline, particularly near river deltas, may be due to agricultural runoff, sedimentation, and turbidity (Ibid). Both maps also show losses in Glover's Atoll, and the Sentinel-2 classification reveals a substantial loss in the Lighthouse Atoll (Figure 9).

There is a pattern of gains in the southern part of the EEZ, close to the coast, and in the shallow water zone located in the north-central region, between the mainland and the reef, in both change detection performed in this set of classification maps.

6. Discussion

Seagrass habitat was widespread throughout the study area, with the coastline having the highest concentration (as shown in Figures 7 and 8). Seagrass meadows were also found alongside the reef, particularly in the west of the reef barrier, which is consistent with previous studies conducted by Rützler & Macintyre in 1982. The presence of seagrass along the reef remained consistent over the years, as observed alongside the Belize Barrier Reef Reserve System (BBRRS). In the northern region, seagrass beds were captured in both classification maps within a larger area. After careful consideration, this may be an overinterpretation related to high turbidity levels.

The elevated NDWI and mNDWI values detected in the center of Turneffe Atoll suggest a thriving seagrass ecosystem. However, the high turbidity levels present in the Atolls may have impacted the classification outcomes. As such, it is possible that the seagrass cover was overestimated in these zones (Carpenter et al., 2022).

The seagrass cover maps presented in this study show a similar level of accuracy for the periods of 2016-2019 and 2020-2022. This consistency can be attributed to the use of a consistent mapping method that relied on detailed training points and pixel-satellite image classification. Despite the challenges posed by the complexity of ecological parameters, the accuracies for seagrass identification were relatively stable across both datasets, with slight improvements observed in the Sentinel-2 data.

Further refinement of the model or inclusion of more training data could lead to improved accuracies. However, it is important to note that there is a certain error rate associated with extracting seagrass beds using the RF model. The use of precise ground truth data obtained directly from the investigation site helped to enhance the reliability and quality of the resultant maps.

For a large proportion of the coastline, an overrepresentation of seagrass is present in both maps (Fig 4). This might be for an underperformance of the turbidity index. Seagrass was mapped in the lagoon, in agreement with other studies (Gaston et al., 2009).

During our land masking efforts, we found that all histograms used for the Otsu-based masking resulted in bi-modal distributions, which allowed for a clear distinction between water and land. However, the deepwater masking process utilizing HSV could not perfectly distinguish deepwater areas, so we included this category in our final classification. To minimize the impact of deepwater, we incorporated bathymetry data available for the zone.

The detectability and visibility of seagrass in satellite imagery are influenced by the attenuation of light in water, and water depth is a crucial factor. To address this, corrections

6. Discussion

are applied to the images to compensate for the effect of the water column. One of the challenges in creating water composites is sunglint, which can cause significant issues when classifying images, as observed in the Sentinel-2 classification. Losses in the northwest vicinity of the shore may be linked to this effect, as noted by Gaston et al. in 2009.

To accurately predict continuous seagrass cover, visual analysis of satellite imagery was utilized to produce the training dataset for classification. However, in-situ data is still necessary for achieving precise results. While the data points were evenly spread throughout the EEZ, specific regions, notably those situated within the Turneffe Atoll, had a higher volume of training points. This was due to these areas having been subject to more in-depth studies, which influenced subsequent image classifications.

The methodology utilized was found to be successful in mapping benthic habitats in the area using two distinct images featuring varying spatial resolutions. Nevertheless, the inclusion of precise data in the model is crucial for achieving improved results in the classification process. This is particularly vital for classifications such as rubble and coral, where the RF algorithm did not perform optimally.

Our approach combines dense and sparse seagrasses into a single classification, which presents a challenge when accurately calculating carbon stocks in the area. Each species has unique carbon sequestration and accumulation characteristics (Hemminga and Duarte, 2000). To refine our findings and accurately determine carbon stocks among seagrasses in the Belizean EEZ, future work should focus on discriminating between seagrass species.

Effective seagrass monitoring relies on habitat mapping and observation of biophysical properties at the appropriate scale (Carpenter et al., 2022). Our analysis showed that the RF classification performed better on Sentinel-2 composites, possibly due to the versatility of the mosaics we created ourselves rather than pre-existing PS.

To address the challenges posed by turbidity, one potential solution would be to evaluate changes in seasonal maps that include both wet and dry seasons in Belize.

6.2. Ecosystem condition: Health assessment of seagrass in Belize in terms of blue carbon

The analysis focused on carbon stock, total net carbon sequestration, and carbon accumulation. These metrics report the capacity of ecosystems to capture and store

6. Discussion

carbon dioxide from the atmosphere (Watts et al., 2014). We focused on these parameters due to the fact they give information about how seagrasses act as a carbon sink.

The difference in spatial resolution between PlanetScope and Sentinel-2 satellites is a critical factor in interpreting the results. PS higher resolution provides more detailed information on a finer scale, which might have resulted in capturing small-scale changes in seagrass cover and, thus, in carbon stocks than S2 due to its coarser resolution. This can lead to higher sums of carbon sequestration and stock in the PS data. However, the consistent maximum values across both datasets suggest that both satellites effectively capture the upper limits of carbon storage potential in the landscape.

The comparison elucidates the complementarity of PS and S2 datasets in monitoring carbon dynamics. While PS offers detailed insights into carbon changes at a finer spatial scale, S2 provides a broader view that can be essential for regional or global-scale analyses.

To assess the condition of carbon on seagrass on the sedimentary OC stock, it is important to examine all stock components, including live and dead aboveground and belowground biomass in the sediment column (Tanaya et al., 2018).

By using a consistent methodology and data sources to generate accounts for multiple time periods, any alterations observed in the accounts can be accurately attributed to legitimate shifts within the ecosystem.

The decrease in seagrass across a broad-scale area of relatively MPA's, and loss of 40% seagrass in some regions during 7 years is alarming. These results are similar to other ones carried out in the area (Gaston et al., 2009). Some changes, however, can be natural, as Gaston et al, 2009 described in the study on the MPA where channels between reefs provide access for ocean-water flux into the lagoon during rising tides. Therefore, this pattern leads us to suggest that the lack of clear ocean water influx may be a limiting factor to seagrass survival in that region.

Our results enhance the importance of preserving this ecosystem in the MPA system in Belize. Although seascape metrics could provide an effective indicator of potential carbon stock, there is a need to determine the appropriate spatio-temporal scale for adequately capturing the biophysical processes influencing the relationship between the spatial configuration of seagrass meadows and carbon sequestration (Simpson et al., 2022).

6. Discussion

The used model assumes that the only change in carbon storage comes from the changes from one cover class to another. Therefore, it is a simplified version that disregards gains or losses over time and does not consider carbon dynamics from one pool to another.

Technical limitations of this model are related to the way it adds the carbon pools, failing to account for changes in the carbon capacity of plants through years. Despite establishing a linear trend for the changes, this could represent a trade off for the model in terms of highly dynamic ecosystem such as seagrass (Lavery et al., 2013).

This accumulation, when juxtaposed with the spatial extension calculated to be approximately 810,202.28 square kilometers sheds light on the critical environmental role played by the area. The increase from 53.91 Mt CO₂e/ha to 128.52 Mt CO₂e/ha between the two epochs underscores the region's significant contribution to mitigating climate change through enhanced carbon storage.

6.3. Fusing EO with biophysical models in an EA framework

This study leverages Earth Observation to quantify the extension of seagrass with biophysical modeling of carbon. Satellite images proved indispensable in determining the spatial location of seagrass, particularly in identifying patterns of carbon (Blume et al., 2023).

In the first stage, we aimed to determine whether seagrass habitat was being lost or gained in the area, understanding its patterns and distribution. Classification maps derived from satellite imagery presented the hotspots for seagrass habitats in the EEZ. Knowing the spatial distribution of seagrass of gains and losses (Figure 9) benefits marine planning and science-based decision-making (Grimm et. al., 2023).

The InVEST Coastal Blue Carbon and Carbon Sequestration and Storage models performed in seagrass help to understand the carbon quantity held by this ecosystem. The carbon maps taken from the model reflect a considerable amount of carbon being storage on these ecosystem, which correspond with other results using the same methodology on different study sites (González-García et. al., 2022) (Montero-Hidalgo et. al, 2023).

This study did not acknowledge the causes and consequences of those changes for the Belizean population. Further studies should address the causes for seagrass conversion, its range, and the impact of this ecosystem's loss on the services it provides to the population. This understanding is crucial for identifying reliable indicators for carbon stock assessments and policies (Macreadie et al., 2014).

6. Discussion

Due to the lack of local data, the accuracy of the model could not be defined precisely. Future work should compare the results from this model to ground-truth data.

The InVEST model demonstrated its efficacy in generating carbon value estimates at different classification map resolutions, encompassing various carbon metrics of the region. This method is transparent and globally applicable, allowing for seamless comparisons with other regions. Setting up further agreements towards the seagrass carbon model is imperative to devise guidelines that safeguard this vital ecosystem. Belize has taken the lead in enforcing conservation measures in its territorial waters, in keeping with its pledge to reduce its carbon footprint (Arkema et al., 2023) (Grimm et al., 2023).

A marine ecosystem classification was developed to optimize the model using high-resolution satellite imagery. This crucial input facilitated the identification of seagrass concentrations (Watts et al., 2014).

Data limitations were one problem in developing this research. Therefore, the data used in this research was taken from a literature review. For the carbon analysis, the information was Tier 1 and Tier 3, where data from other regions did not consider specific species and location variability. Integrating additional field data could further enhance the development of classification algorithms and improve carbon assessment.

Alongside the Coastal Blue Carbon model, this study utilized the Carbon Sequestration and Storage model to determine the quantity of carbon sequestered and stored in sediments. The resulting maps exhibit congruity between the findings of both models. Although this model has its drawbacks, including its failure to consider fluxes between ecosystems and its reliance on linear growth and exponential sequestration assumptions until the ecosystem is disrupted, it requires minimal parameters to execute. Nevertheless, it served as a foundation for analyzing ecosystem fluctuations.

These findings indicate that bioregional and geomorphic characteristics may not reliably forecast soil organic carbon (Corg) reserves, suggesting the necessity for site-specific assessments grounded in local environmental conditions for Blue Carbon initiatives and greenhouse gas accounting (Mazarrasa et al., 2021).

Guidelines for precise quantification of seagrass carbon stock have been established, with the aim of integrating it into national greenhouse gas inventories (GHG) (Arkema et al., 2023). Examining the ecological characteristics of seagrass and evaluating the potential of remote sensing techniques with other methods are integral parts of this task.

6. Discussion

Future studies will focus on improving the adaptability of the modeling techniques to facilitate their use across regional and national scales. Additionally, developing multitemporal composites with finer temporal resolutions will enable the generation of more extensive and comprehensive time series. This enhancement will support a more dependable analysis of patterns within the year, mainly by creating seasonal maps that capture the variations in turbidity index during Belize's wet and dry seasons.

Assessing the condition of a system may not only involve carbon but also other biophysical factors that are at play in seagrass ecosystems. Based on the study's objective, coupled biophysical models of contaminant concentration, water quality, and Chlorophyll-a content can help determine a correlation between ecosystem condition and its capacity to promote carbon sequestration (United Nations, 2022).

This study serves as a first step into the carbon modelling at Belize. With the required data at hand, more epochs and even scenarios could be used to predict the future carbon levels. By incorporating scenarios such as Business-As-Usual, Conservation, No-Net-Loss, and Intermediate-Conservation-Efforts, we could gain a better understanding of the future blue carbon capacity of seagrass in Belize, as stated in the works of Montero-Hidalgo et al. (2023) and González-García (2022). This research can provide direction for conservation projects that aim to preserve seagrass meadows in the region. To translate satellite-derived ecological characteristics into metrics relevant to carbon stock and sequestration rate estimates. Additional assets, such as distance to the water, fisheries, and protected areas, will be studied and parameterised with biophysical variables under different management scenarios, including business-as-usual, conservation, and sustainable development.

It is important to note that our research only focused on the first two stages of the Ecosystem Accounting Framework. By including steps such as Ecosystem Service and Asset Account, a defined monetary value can be assigned to preserving these ecosystems, as mentioned in the works of Montero-Hidalgo et. al. (2023) and González-García et. al. (2022). This monetary value can be crucial in determining efforts for implementing projects that aim to preserve this vital ecosystem (Blume et al., 2023).

7. Conclusion

The importance of seagrass habitats in capturing organic carbon makes them a crucial element in supporting efforts to mitigate climate change. To better understand the carbon stocks in seagrass in Belize, we utilized the SEEA-EA framework phases of ecosystem extent in conjunction with Earth Observation techniques and ecosystem conditions to model model carbon dynamics.

In order to determine changes in seagrass between the two periods, we analyzed spatial fluxes and compared C content in the region using the Coastal Blue Carbon model of InVEST.

Our research shows a concerning loss of this important ecosystem in the study period, particularly in the northern region of Belize's EEZ. Moreover, there are also gains of seagrass around the study area.

The analysis focused on carbon stock, total net carbon sequestration, and carbon accumulation derived from two different satellites. This analysis showed a higher carbon content taken from the PS composite map. However, both classification maps show a constant sequestration of carbon in the area of study.

By utilizing remote sensing-based maps and biophysical carbon models, we were able to generate highly accurate carbon estimates, making this approach especially useful in areas where C stocks data is not readily available.

This pilot research demonstrated the potential of the InVEST CBC in quantifying the carbon content of the Belizean seagrass beds. With the setup of this framework for a benthic application of InVEST, researchers, conservation managers and policy makers will not only be able to monitor their seagrass carbon stocks and forecasts, but also any other possible biophysical parameters of importance to seagrasses and other benthic habitats.

8. References

- Arkema, K. K., Delevaux, J. M. S., Silver, J. M., Winder, S. G., Schile-Beers, L. M., Bood, N., Crooks, S., Douthwaite, K., Durham, C., Hawthorne, P. L., Hickey, T., Mattis, C., Rosado, A., Ruckelshaus, M., von Unger, M., & Young, A. (2023). Evidence-based target setting informs blue carbon strategies for nationally determined contributions. *Nature Ecology & Evolution*, 7(7), Article 7. <https://doi.org/10.1038/s41559-023-02081-1>
- Atwood, T. B., Witt, A., Mayorga, J., Hammill, E., & Sala, E. (2020). Global Patterns in Marine Sediment Carbon Stocks. *Frontiers in Marine Science*, 7. <https://www.frontiersin.org/articles/10.3389/fmars.2020.00165>
- Bai, J., Li, Y., Chen, S., Du, J., & Wang, D. (2023). Long-time monitoring of seagrass beds on the east coast of Hainan Island based on remote sensing images. *Ecological Indicators*, 157, 111272. <https://doi.org/10.1016/j.ecolind.2023.111272>
- Blume, A., Pertiwi, A. P., Lee, C. B., & Traganos, D. (2023). Bahamian seagrass extent and blue carbon accounting using Earth Observation. *Frontiers in Marine Science*, 10. <https://www.frontiersin.org/articles/10.3389/fmars.2023.1058460>
- Burgos, Amanda, et al. "WWF Position and Guidance on Voluntary Purchases of Carbon Credits." Belize Scorecard 2017, World Wildlife Fund, c402277.ssl.cf1.rackcdn.com/publications/1310/files/original/WWF_position_and_guidance_on_corporate_use_of_voluntary_carbon_credits_EXTERNAL_VERSION_11_October_2019_v1.2.pdf?1591194127. Accessed 11 Oct. 2023.
- Busch, J., Greer, L., Harbor, D., Wirth, K., Lescinsky, H., Curran, A., & de Beurs, K. (2016). Quantifying exceptionally large populations of *Acropora* spp. Corals off Belize using sub-meter satellite imagery classification. *Bulletin of Marine Science -Miami*, 92, 265–283. <https://doi.org/10.5343/bms.2015.1038>
- Carlson, R. R., Evans, L. J., Foo, S. A., Grady, B. W., Li, J., Seeley, M., Xu, Y., & Asner, G. P. (2021). Synergistic benefits of conserving land-sea ecosystems. *Global*

Ecology and Conservation, 28, e01684.

<https://doi.org/10.1016/j.gecco.2021.e01684>

Carpenter, S., Byfield, V., Felgate, S. L., Price, D. M., Andrade, V., Cobb, E., Strong, J., Lichtschlag, A., Brittain, H., Barry, C., Fitch, A., Young, A., Sanders, R., & Evans, C. (2022). Using Unoccupied Aerial Vehicles (UAVs) to Map Seagrass Cover from Sentinel-2 Imagery. *Remote Sensing*, 14(3), Article 3. <https://doi.org/10.3390/rs14030477>

Delwart, S. (n.d.). ESA Standard Document. 1.

do Amaral Camara Lima, M., Bergamo, T. F., Ward, R. D., & Joyce, C. B. (2023). A review of seagrass ecosystem services: Providing nature-based solutions for a changing world. *Hydrobiologia*, 850(12), 2655–2670. <https://doi.org/10.1007/s10750-023-05244-0>

Donchyts, G., Schellekens, J., Winsemius, H., Eisemann, E., & Van de Giesen, N. (2016). A 30 m Resolution Surface Water Mask Including Estimation of Positional and Thematic Differences Using Landsat 8, SRTM and OpenStreetMap: A Case Study in the Murray-Darling Basin, Australia. *Remote Sensing*, 8(5), Article 5. <https://doi.org/10.3390/rs8050386>

Duarte, C. M. (2002). The future of seagrass meadows. *Environmental Conservation*, 29(2), 192–206. <https://doi.org/10.1017/S0376892902000127>

Duarte, C. M., & Cebrián, J. (1996). The fate of marine autotrophic production. *Limnology and Oceanography*, 41(8), 1758–1766. <https://doi.org/10.4319/lo.1996.41.8.1758>

Duarte, C. M., & Chiscano, C. L. (1999). Seagrass biomass and production: A reassessment. *Aquatic Botany*, 65(1), 159–174. [https://doi.org/10.1016/S0304-3770\(99\)00038-8](https://doi.org/10.1016/S0304-3770(99)00038-8)

Duarte, C. M., Middelburg, J. J., & Caraco, N. (2005). Major role of marine vegetation on the oceanic carbon cycle. *Biogeosciences*, 2(1), 1–8. <https://doi.org/10.5194/bg-2-1-2005>

- Fourqurean, J. W., Duarte, C. M., Kennedy, H., Marbà, N., Holmer, M., Mateo, M. A., Apostolaki, E. T., Kendrick, G. A., Krause-Jensen, D., McGlathery, K. J., & Serrano, O. (2012). Seagrass ecosystems as a globally significant carbon stock. *Nature Geoscience*, 5(7), Article 7. <https://doi.org/10.1038/ngeo1477>
- Gago González, M. (2015). Catchment influences on the hydrological flows to lake terra alta (Linhares, ES, Brazil) and ecohydrology perspectives. <https://core.ac.uk/download/216330527.pdf>
- Gallegos, M., Merino, M., Rodriguez, A., Marba, N., & Duarte, C. (1994). Growth patterns and demography of pioneer Caribbean seagrasses *Halodule wrightii* and *Syringodium filiforme*. *Marine Ecology Progress Series*, 109, 99–104. <https://doi.org/10.3354/meps109099>
- Garrard, S. L., & Beaumont, N. J. (2014). The effect of ocean acidification on carbon storage and sequestration in seagrass beds; a global and UK context. *Marine Pollution Bulletin*, 86(1), 138–146. <https://doi.org/10.1016/j.marpolbul.2014.07.032>
- Gaston, G. R., Easson, C., Easson, G., Janaskie, J., & Ballas, M. A. (2009). Seagrass Loss in Belize: Studies of Turtlegrass (*Thalassia testudinum*) Habitat Using Remote Sensing and Ground-Truth Data. *Gulf and Caribbean Research*, 21. <https://doi.org/10.18785/gcr.2101.03>
- J. Gibson, M. McField, W. Heyman, S. Wells, J. Carter, G. Sedberry.(2004). Belize's evolving system of marine reserves. *Marine Reserves: A Guide to Science, Design and Use*, 287-316.
- Grimm, K. E., Archibald, J. L., Bonilla-Anariba, S. E., Bood, N., & Canty, S. W. J. (2023). Framework for fostering just and equitable seagrass policy, management, and social-ecological outcomes: Lessons learned from Belizean marine resource managers. *Marine Policy*, 152, 105606. <https://doi.org/10.1016/j.marpol.2023.105606>
- Gischler, E. (2011). Belize Barrier and Atoll Reefs. In D. Hopley (Ed.), *Encyclopedia of Modern Coral Reefs: Structure, Form and Process* (pp. 112–118). Springer

Netherlands. https://doi.org/10.1007/978-90-481-2639-2_45

Gonzalez-Garcia, Alberto & Arias, Marina & Garcia-Tiscar, Susana & Alcorlo, Paloma & Santos-Martín, Fernando, 2022. "National blue carbon assessment in Spain using InVEST: Current state and future perspectives," *Ecosystem Services*, Elsevier, vol. 53(C).

Grech, A., Chartrand-Miller, K., Erftemeijer, P., Fonseca, M., McKenzie, L., Rasheed, M., Taylor, H., & Coles, R. (2012). A comparison of threats, vulnerabilities and management approaches in global seagrass bioregions. *Environmental Research Letters*, 7(2), 024006. <https://doi.org/10.1088/1748-9326/7/2/02400>

Hein, L. (2014). *Biophysical Modelling and Analysis of Ecosystem Services in an Ecosystem Accounting Context*.

Hejnowicz, A. P., Kennedy, H., Rudd, M. A., & Huxham, M. R. (2015). Harnessing the climate mitigation, conservation and poverty alleviation potential of seagrasses: Prospects for developing blue carbon initiatives and payment for ecosystem service programmes. *Frontiers in Marine Science*, 2. <https://www.frontiersin.org/articles/10.3389/fmars.2015.00032>

Hemminga, M. A., & Duarte, C. M. (2000). *Seagrass Ecology*. Cambridge University Press. <https://doi.org/10.1017/CBO9780511525551>

Hendriks, I., Sintes, T., Bouma, T., & Duarte, C. (2008). Experimental assessment and modeling evaluation of the effects of the seagrass *Posidonia oceanica* on flow and particle trapping. *Marine Ecology Progress Series*, 356, 163–173. <https://doi.org/10.3354/meps07316>

IPCC, 2023: Annex I: Glossary [Reisinger, A., D. Cammarano, A. Fischlin, J.S. Fuglestedt, G. Hansen, Y. Jung, C. Ludden, V. Masson-Delmotte, R. Matthews, J.B.K Mintenbeck, D.J. Orendain, A. Pirani, E. Poloczanska, and J. Romero (eds.)]. In: *Climate Change 2023: Synthesis Report. Contribution of Working Groups I, II and III to the Sixth Assessment Report of the Intergovernmental Panel*

- on Climate Change [Core Writing Team, H. Lee and J. Romero (eds.)]. IPCC, Geneva, Switzerland, pp. 119-130, doi: 10.59327/IPCC/AR6-9789291691647.002.
- Johannessen, S. (2023). How to quantify blue carbon sequestration rates in seagrass meadow sediment: Geochemical method and troubleshooting. *Carbon Footprints*, 2. <https://doi.org/10.20517/cf.2023.37>
- Kay, S., Hedley, J. and Lavender, S. (2009). Sun Glint Correction of High and Low Spatial Resolution Images of Aquatic Scenes: a Review of Methods for Visible and Near-Infrared Wavelengths, *Remote Sensing* 1(4): 697–730. DOI: 10.3390/rs1040697.
- Kennedy, H., Beggins, J., Duarte, C. M., Fourqurean, J. W., Holmer, M., Marbà, N., & Middelburg, J. J. (2010). Seagrass sediments as a global carbon sink: Isotopic constraints. *Global Biogeochemical Cycles*, 24(4). <https://doi.org/10.1029/2010GB003848>
- Laffoley, D., & Grimsditch, G. D. (2009). *The Management of Natural Coastal Carbon Sinks*. IUCN.
- Lavery, P. S., Mateo, M.-Á., Serrano, O., & Rozaimi, M. (2013). Variability in the Carbon Storage of Seagrass Habitats and Its Implications for Global Estimates of Blue Carbon Ecosystem Service. *PLOS ONE*, 8(9), e73748. <https://doi.org/10.1371/journal.pone.0073748>
- Lee, C. B., Martin, L., Traganos, D., Antat, S., Baez, S. K., Cupidon, A., Faure, A., Harlay, J., Morgan, M., Mortimer, J. A., Reinartz, P., & Rowlands, G. (2023). Mapping the National Seagrass Extent in Seychelles Using PlanetScope NICFI Data. *Remote Sensing*, 15(18), Article 18. <https://doi.org/10.3390/rs15184500>
- Li, J., Fabina, N. S., Knapp, D. E., & Asner, G. P. (2020). The Sensitivity of Multi-spectral Satellite Sensors to Benthic Habitat Change. *Remote Sensing*, 12(3), Article 3. <https://doi.org/10.3390/rs12030532>
- Lyzenga, D. R., Malinas, N. P., & Tanis, F. J. (2006). Multispectral bathymetry using a simple physically based algorithm. *IEEE Transactions on Geoscience and Remote Sensing*, 44(8), 2251–2259. <https://doi.org/10.1109/TGRS.2006.872909>

- Macreadie, P. I., Baird, M. E., Trevathan-Tackett, S. M., Larkum, A. W. D., & Ralph, P. J. (2014). Quantifying and modelling the carbon sequestration capacity of seagrass meadows – A critical assessment. *Marine Pollution Bulletin*, 83(2), 430–439. <https://doi.org/10.1016/j.marpolbul.2013.07.038>
- Maxwell, T. L., Rovai, A. S., Adame, M. F., Adams, J. B., Álvarez-Rogel, J., Austin, W. E. N., Beasy, K., Boscutti, F., Böttcher, M. E., Bouma, T. J., Bulmer, R., Burden, A., Burke, S., Camacho, S. M. G., Chaudhary, D. R., Chmura, G. L., Copertino, M., Cott, G. M., Craft, C., . . . Worthington, T. A. (2023). Global dataset of soil organic carbon in tidal marshes. *Scientific Data*. <https://doi.org/10.1038/s41597-023-02633-x>
- Mazarrasa, I., Lavery, P., Duarte, C. M., Lafratta, A., Lovelock, C. E., Macreadie, P. I., Samper-Villarreal, J., Salinas, C., Sanders, C. J., Trevathan-Tackett, S., Young, M., Steven, A., & Serrano, O. (2021). Factors Determining Seagrass Blue Carbon Across Bioregions and Geomorphologies. *Global Biogeochemical Cycles*, 35(6), e2021GB006935. <https://doi.org/10.1029/2021GB006935>
- McKenzie, L. J., Nordlund, L. M., Jones, B. L., Cullen-Unsworth, L. C., Roelfsema, C., & Unsworth, R. K. F. (2020). The global distribution of seagrass meadows. *Environmental Research Letters*, 15(7), 074041. <https://doi.org/10.1088/1748-9326/ab7d06>
- Mcleod, E., Chmura, G. L., Bouillon, S., Salm, R., Björk, M., Duarte, C. M., Lovelock, C. E., Schlesinger, W. H., & Silliman, B. R. (2011). A blueprint for blue carbon: Toward an improved understanding of the role of vegetated coastal habitats in sequestering CO₂. *Frontiers in Ecology and the Environment*, 9(10), 552–560. <https://doi.org/10.1890/110004>
- Montero-Hidalgo M, Tuya F, Otero-Ferrer F, Haroun R, Santos-Martín F. Mapping and assessing seagrass meadows changes and blue carbon under past, current, and future scenarios. *Sci Total Environ*. 2023 May 10;872:162244. doi: 10.1016/j.scitotenv.2023.162244. Epub 2023 Feb 14. PMID: 36796703.

- Natural Capital Project, 2024. InVEST 3.14.1. Stanford University, University of Minnesota, Chinese Academy of Sciences, The Nature Conservancy, World Wildlife Fund, Stockholm Resilience Centre and the Royal Swedish Academy of Sciences. <https://naturalcapitalproject.stanford.edu/software/invest>
- NICFI_User_Guide_EN.pdf. (n.d.). Retrieved February 15, 2024, from https://assets.planet.com/docs/NICFI_User_Guide_EN.pdf
- Pertiwi, A. P., Lee, C. B., & Traganos, D. (2021). Cloud-Native Coastal Turbid Zone Detection Using Multi-Temporal Sentinel-2 Data on Google Earth Engine. *Frontiers in Marine Science*, 8. <https://www.frontiersin.org/articles/10.3389/fmars.2021.699055>
- Pham, T. D., Xia, J., Ha, N. T., Bui, D. T., Le, N. N., & Tekeuchi, W. (2019). A Review of Remote Sensing Approaches for Monitoring Blue Carbon Ecosystems: Mangroves, Seagrasses and Salt Marshes during 2010–2018. *Sensors*, 19(8), Article 8. <https://doi.org/10.3390/s19081933>
- Planet. (July de 2022). NICFI Satellite Data Program User guide. Retrieved February 15, 2024, from Planet:: https://assets.planet.com/docs/NICFI_User_Guide_EN.pdf
- Qiu, G.-L., Lin, H.-J., Li, Z.-S., Fan, H.-Q., Zhou, H.-L., & Liu, G.-H. (2014). [Seagrass ecosystems: Contributions to and mechanisms of carbon sequestration]. *Ying Yong Sheng Tai Xue Bao = The Journal of Applied Ecology*, 25(6), 1825–1832.
- Roelfsema, C., Kovacs, E. M., Saunders, M. I., Phinn, S., Lyons, M., & Maxwell, P. (2013). Challenges of remote sensing for quantifying changes in large complex seagrass environments. *Estuarine, Coastal and Shelf Science*, 133, 161–171. <https://doi.org/10.1016/j.ecss.2013.08.026>
- Roelfsema, C., Phinn, S., Udy, N., & Maxwell, P. (2009). An Integrated Field and Remote Sensing Approach for Mapping Seagrass Cover, Moreton Bay, Australia. *Spatial Science*, 54. <https://doi.org/10.1080/14498596.2009.9635166>
- Rützler, Klaus and Macintyre, Ian G. 1982. The Atlantic barrier reef ecosystem at Carrie

- Bow Cay, Belize, 1: Structure and Communities. Smithsonian Institution Press.
<https://doi.org/10.5479/si.01960768.12.539>
- Schill, S. R., McNulty, V. P., Pollock, F. J., L uthje, F., Li, J., Knapp, D. E., Kington, J. D., McDonald, T., Raber, G. T., Escovar-Fadul, X., & Asner, G. P. (2021). Regional High-Resolution Benthic Habitat Data from Planet Dove Imagery for Conservation Decision-Making and Marine Planning. *Remote Sensing*, 13(21), Article 21. <https://doi.org/10.3390/rs13214215>
- Serrano, O., G omez-L opez, D. I., S anchez-Valencia, L., Acosta-Chaparro, A., Navas-Camacho, R., Gonz alez-Corredor, J., Salinas, C., Masque, P., Bernal, C. A., & Marb a, N. (2021). Seagrass blue carbon stocks and sequestration rates in the Colombian Caribbean. *Scientific Reports*, 11(1), Article 1. <https://doi.org/10.1038/s41598-021-90544-5>
- Serrano, O., Lovelock, C. E., B. Atwood, T., Macreadie, P. I., Canto, R., Phinn, S., Arias-Ortiz, A., Bai, L., Baldock, J., Bedulli, C., Carnell, P., Connolly, R. M., Donaldson, P., Esteban, A., Ewers Lewis, C. J., Eyre, B. D., Hayes, M. A., Horwitz, P., Hutley, L. B., ... Duarte, C. M. (2019). Australian vegetated coastal ecosystems as global hotspots for climate change mitigation. *Nature Communications*, 10(1), 4313. <https://doi.org/10.1038/s41467-019-12176-8>
- Short, F., Carruthers, T., Dennison, W., & Waycott, M. (2007). Global seagrass distribution and diversity: A bioregional model. *Journal of Experimental Marine Biology and Ecology*, 350(1), 3–20. <https://doi.org/10.1016/j.jembe.2007.06.012>
- Short, F. T., Koch, E. W., Creed, J. C., Magalh aes, K. M., Fernandez, E., & Gaeckle, J. L. (2006). SeagrassNet monitoring across the Americas: Case studies of seagrass decline. *Marine Ecology*, 27(4), 277–289. <https://doi.org/10.1111/j.1439-0485.2006.00095.x>
- Simpson, J., Bruce, E., Davies, K. P., & Barber, P. (2022). A Blueprint for the Estimation of Seagrass Carbon Stock Using Remote Sensing-Enabled Proxies. *Remote Sensing*, 14(15), Article 15. <https://doi.org/10.3390/rs14153572>

- Stankovic, M., Ambo-Rappe, R., Carly, F., Dangan-Galon, F., Fortes, M. D., Hossain, M. S., Kiswara, W., Van Luong, C., Minh-Thu, P., Mishra, A. K., Noiraksar, T., Nurdin, N., Panyawai, J., Rattanachot, E., Rozaimi, M., Soe Htun, U., & Prathep, A. (2021). Quantification of blue carbon in seagrass ecosystems of Southeast Asia and their potential for climate change mitigation. *Science of The Total Environment*, 783, 146858. <https://doi.org/10.1016/j.scitotenv.2021.146858>
- SUHET. (1 de september de 2014). Sentinel -2 User Handbook. Retrieved February 15, 2024, from The European Space Agency: https://sentinel.esa.int/documents/247904/685211/Sentinel-2_User_Handbook
- Tanaya, T., Watanabe, K., Yamamoto, S., Hongo, C., Kayanne, H., & Kuwae, T. (2018). Contributions of the direct supply of belowground seagrass detritus and trapping of suspended organic matter to the sedimentary organic carbon stock in seagrass meadows. *Biogeosciences*, 15(13), 4033–4045. <https://doi.org/10.5194/bg-15-4033-2018>
- Traganos, D., & Reinartz, P. (2018a). Machine learning-based retrieval of benthic reflectance and *Posidonia oceanica* seagrass extent using a semi-analytical inversion of Sentinel-2 satellite data. *International Journal of Remote Sensing*, 39, 1–25. <https://doi.org/10.1080/01431161.2018.1519289>
- Traganos, D., & Reinartz, P. (2018b). Machine learning-based retrieval of benthic reflectance and *Posidonia oceanica* seagrass extent using a semi-analytical inversion of Sentinel-2 satellite data. *International Journal of Remote Sensing*, 39(24), 9428–9452. <https://doi.org/10.1080/01431161.2018.1519289>
- Tussenbroek, B. I. van, Cortés, J., Collin, R., Fonseca, A. C., Gayle, P. M. H., Guzmán, H. M., Jácome, G. E., Juman, R., Koltjes, K. H., Oxenford, H. A., Rodríguez-Ramirez, A., Samper-Villarreal, J., Smith, S. R., Tschirky, J. J., & Weil, E. (2014). Caribbean-Wide, Long-Term Study of Seagrass Beds Reveals Local Variations, Shifts in Community Structure and Occasional Collapse. *PLOS ONE*, 9(3), e90600. <https://doi.org/10.1371/journal.pone.0090600>

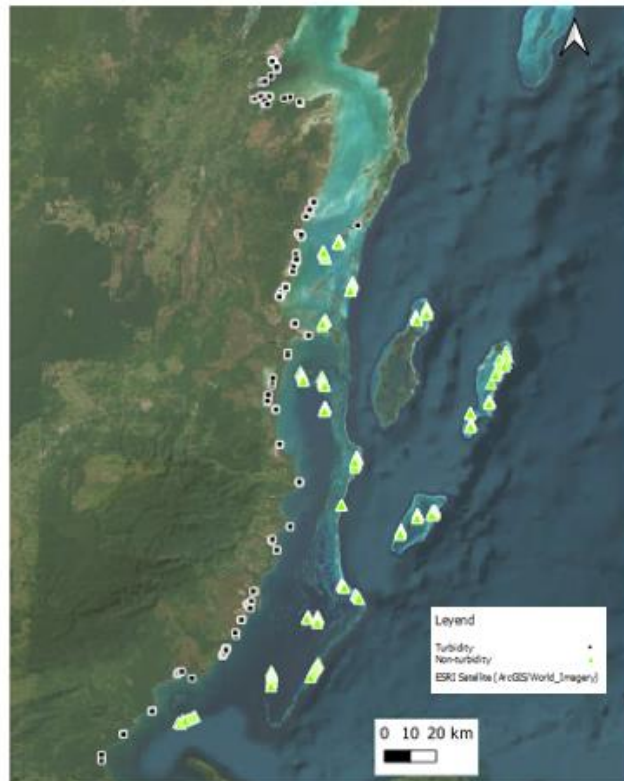
- United Nations (2022). Guidelines on Biophysical Modelling for Ecosystem Accounting. United Nations Department of Economic and Social Affairs, Statistics Division, New York. Retrieved February 15, 2024, from System of Environmental Economic Accounting:
https://seea.un.org/sites/seea.un.org/files/publications/guidancebiomodelling_v36_30032022_web.pdf
- UNESCO (2023). Boundaries of UNESCO World Heritage Marine Sites (v02). Available online at <https://www.marineregions.org/>. <https://doi.org/10.14284/592>
- UNEP-WCMC, WorldFish Centre, WRI, TNC (2021). Global distribution of warm-water coral reefs, compiled from multiple sources including the Millennium Coral Reef Mapping Project. Version 4.1. Includes contributions from IMaRS-USF and IRD (2005), IMaRS-USF (2005) and Spalding et al. (2001). Cambridge (UK): UN Environment World Conservation Monitoring Centre. Data DOI: <https://doi.org/10.34892/t2wk-5t34>
- UNEP-WCMC and IUCN (2024), Protected Planet: The World Database on Protected Areas (WDPA) and World Database on Other Effective Area-based Conservation Measures (WD-OECM) [Online], January 2024, Cambridge, UK: UNEP-WCMC and IUCN. Available at: www.protectedplanet.net.
- Veettil, B. K., Ward, R. D., Lima, M. D. A. C., Stankovic, M., Hoai, P. N., & Quang, N. X. (2020). Opportunities for seagrass research derived from remote sensing: A review of current methods. *Ecological Indicators*, 117, 106560. <https://doi.org/10.1016/j.ecolind.2020.106560>.
- Wabnitz, C. C., Andréfouët, S., Torres-Pulliza, D., Müller-Karger, F. E., & Kramer, P. A. (2008). Regional-scale seagrass habitat mapping in the Wider Caribbean region using Landsat sensors: Applications to conservation and ecology. *Remote Sensing of Environment*, 112(8), 3455–3467. <https://doi.org/10.1016/j.rse.2008.01.020>
- Watts, J. D., Kimball, J. S., Parmentier, F. J. W., Sachs, T., Rinne, J., Zona, D., ... & Aurela,

M. (2014). A satellite data driven biophysical modeling approach for estimating northern peatland and tundra CO₂ and CH₄ fluxes. *Biogeosciences*, 11(7), 1961-1980.

World Wide Fund for Nature. (10 de October de 2019). *WWF position and guidance on voluntary purchases of carbon credits*. Retrieved February 15, 2024, from World Wide Fund for Nature: https://files.worldwildlife.org/wwfmsprod/files/Publication/file/773q5lvbf0_WWF_position_and_guidance_on_corporate_use_of_voluntary_carbon_credits_EXTERNAL_VERSION_11_October_2019_v1.2.pdf?_ga=2.207621716.750216319.1709778120-540768202.1709778120

Appendix

- A. Points for turbidity index. A total of 180 points represent locations of turbidity alongside the coastline, with 160 points for training in black and 20 points for validation in green. Turbidity areas example alongside the shore



B. Classification map PlanetScope

| | PS 2016-2019 | | PS 2020-2022 | |
|----------------------|---------------------|---------------|---------------------|---------------|
| | PA | User Accuracy | PA | User Accuracy |
| Sand | 84.94 | 82.2 | 80.69 | 84.6 |
| Seagrass | 65.16 | 79.9 | 65.54 | 79.4 |
| Rubble | 70.58 | 23.1 | 77.64 | 24.52 |
| Coral / Algae | 49.76 | 69.8 | 54.97 | 67.0 |
| Overall | 0.59 | | 0.57 | |

C. Classification map Sentinel-2 L1C

| | S2 2016-2019 | | S2 2020-2022 | |
|----------------------|---------------------|---------------|---------------------|---------------|
| | PA | User Accuracy | PA | User Accuracy |
| Sand | 78.08 | 81.53 | 80.38 | 84.62 |
| Seagrass | 66.68 | 81.59 | 65.71 | 79.44 |
| Rubble | 76.83 | 68.11 | 75.61 | 67.03 |
| Coral / Algae | 54.03 | 25.45 | 54.03 | 24.52 |
| Overall | 0.60 | | 0.61 | |

D. Biophysical data form CBC model

| Parameter | PS Min Value | PS Max Value | PS Sum (10 ⁹) | PS Mean Value | PS Std Deviation | S2 Min Value | S2 Max Value | S2 Sum (10 ⁹) | S2 Mean Value | S2 Std Deviation |
|--|--------------|--------------|---------------------------|---------------|------------------|--------------|--------------|---------------------------|---------------|------------------|
| Carbon Stock (2016) | 0 | 53.92 | 6.48 | 22.34 | 26.56 | 0 | 53.92 | 1.89 | 23.34 | 26.72 |
| Carbon Stock (2022) | 0 | 128.52 | 15.44 | 52.62 | 63.20 | 0 | 128.52 | 4.51 | 55.58 | 63.67 |
| Total Net Carbon Sequestration (2016 - 2022) | 0 | 74.60 | 8.96 | 30.90 | 36.75 | 0 | 74.60 | 2.62 | 32.29 | 36.96 |
| Carbon Accumulation (2016 - 2022) | 0 | 74.60 | 8.96 | 30.90 | 36.75 | 0 | 74.60 | 2.62 | 32.29 | 36.96 |

Values in Mt CO₂e/ha